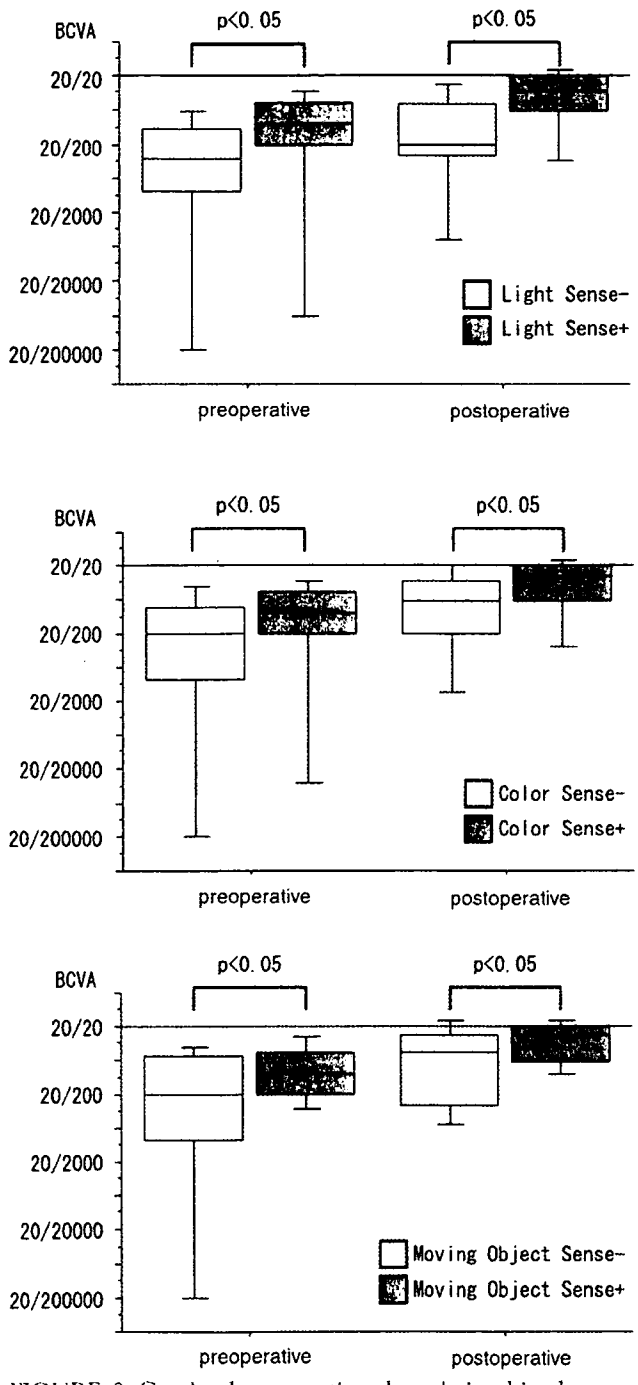

FIGURE 2. Graphs demonstrating the relationships between patients' visual sensations during pars plana vitrectomy under retrobulbar anesthesia such as light, color, and moving object, and preoperative or postoperative visual acuity. (Top) Patients who experienced light had better preoperative visual acuity (mean visual acuity, 0.09; n = 91) compared with patients without light sensation (mean visual acuity, 0.03; n = 10; P = .0235). The postoperative visual acuity in patients who experienced light (mean visual acuity, 0.39; n = 85) is better than that in patients who did not experience light during surgery (mean visual acuity, 0.39; n = 10; P = .0048). (Middle) Patients who experienced color (mean visual acuity, 0.10; n = 73) had better preoperative visual acuity compared with patients who did not see color (mean visual acuity, 0.05; n = 28; P = .0427). The postoperative visual acuity in patients who experienced color (mean visual acuity, 0.44; n = 68) was better than that in patients who did not experience color during surgery (mean visual acuity, 0.15; n = 27; P = .0125). (Bottom) Patients who saw moving objects had better preoperative visual acuity (mean visual acuity, 0.15; n = 47) compared with patients who did not see a moving object (mean visual acuity, 0.04; n = 54; P = .0098). The postoperative visual acuity in patients who saw a moving object (mean visual acuity, 0.58; n = 50) was better than that of patients who did not see any moving object during surgery (mean visual acuity, 0.17; n = 45; P = .0011). BCVA = best-corrected visual acuity; preoperative = before surgery; postoperative = after surgery. Visual acuity of 'counting fingers' and 'hand motion' were converted to 20/2000 and 20/20000, respectively, when the statistical evaluation was made according to the previous report*. *Holladay JT. Visual acuity measurements. J Cataract Refract Surg 2004;30:287–290.

ogenous retinal detachment with macular involvement, submacular hemorrhage, or macular hole, were less likely to experience clear visual sensations. The area of the retinal detachment also may have an influence on some visual sensations. It is possible that our study failed to find a significant correlation because of the small sample number. Because there are many factors that can affect the visual sensations, it is difficult to determine which factors are significant.

It was interesting that a significant correlation was found between the preoperative or postoperative visual acuity and intraoperative visual sensation. Great care is needed to interpret this, and it cannot be expanded directly because the intraoperative visual sensation may predict postoperative visual acuity. Patients who reported intraoperative sensation for not only light but also colors or moving objects, which are perceived mainly by the cone system, showed significantly better postoperative visual acuity. This suggests that the intraoperative visual sensation is highly correlated with the macular function of the patient.

During the preoperative explanation of vitrectomy to patients, extensive technical information about the preoperative and postoperative management is given, and less attention is paid to the intraoperative experiences. Visual sensations during surgery are important determinants of patient satisfaction with any anesthetic technique. In previous studies on retained visual sensations during cataract surgery, a considerable number of the patients (3.0% to 15.4%)[1–9,17] found their visual experience to be frightening. In this study, only six patients reported the visual sensation to be frightening. This small number may explain why we could not find any significant clinical characteristics of these patients. In our study, most patients reported that they were not uncomfortable during the surgery, and some even said they enjoyed the procedure

TABLE 5. Previous Literature Reports of Subjective Experience During Cataract Surgery under Retrobulbar Anesthesia

	Au Eong and Associates, 2000[3]	Chung and Associates, 2004[7]*	Rengaraj and Associates, 2004[8]	Sugisaka and Associates, 2007†
Patient demographics				
No. of patients	70	41	150	101
Age (mean ± SD), yrs	Mean, 65.1 (range, 37 to 87)	75.0 ± 7.8	57.2 ± 8.0	62.2 ± 11.9
Gender	Male, 39; female, 31	Male, 22; female, 19	Male, 76; female, 74	Male, 56; female, 45
Visual perception				
Light	59 (84.3)	39 (95.1)	136 (90.7)	91 (90.1)
Color	39 (55.7)	36 (87.8)	92 (61.3)	73 (72.3)
Details of color perception				
Red	23 (32.9)		18 (19.6)	12 (11.9)
Blue	17 (24.3)		42 (45.7)	17 (16.8)
Yellow	12 (17.1)		21 (23.8)	18 (17.8)
Green	7 (10.0)		5 (5.4)	2 (2.0)
Orange	1 (1.4)		0 (0)	13 (12.9)
Rainbow	8 (11.4)		1 (1.1)	5 (5.0)
White				25 (24.8)
Brown				5 (5.0)
Can't specify			5 (5.4)	12 (11.9)
Flash	35 (50.0)		65 (43.3)	
Movement or moving object	34 (48.6)	27 (65.9)	52 (34.7)	57 (56.4)
Instrument	12 (17.1)		27 (18.0)	54 (53.5)
Fingers or hands	11 (15.7)			9 (8.9)
Fear	5 (7.1)		14 (9.3)	6 (5.9)

SD = standard deviation.

Data are shown as number (%) unless otherwise indicated.

*Regional anesthesia: retrobulbar anesthesia or peribulbar anesthesia.

†This is the current study and deals with visual sensation during vitreous surgery, not cataract surgery.

even though the sensations were totally new experiences. However, such intraoperative sensations can be stressful and even frightening, especially if they are unexpected in some. Therefore, we recommend that the preoperative counseling should include information about the possibility of intraoperative visual sensations that may be experienced. We also want to emphasize that this study confirmed that some intraoperative communication with the patients may help to avoid upsetting patients and may help them to feel assured.

THE AUTHORS INDICATE NO FINANCIAL SUPPORT OR FINANCIAL CONFLICT OF INTEREST. INVOLVED IN DESIGN OF STUDY (K.Sh., M.I.); conduct of study (K.Sh., K.T., M.I.); collection and analysis of the data (E.S., K.Sh., S.I., Y.I., Y.O., H.S., K.Su., M.I.); literature search (E.S., K.Sh.); and statistical performance (K.Sh.). The procedures used conformed to the tenets of the Declaration of Helsinki, and informed consent was obtained after an explanation of the procedures from each individual who participated. Regional ethics committee approval was not required for this study.

REFERENCES

1. Murdoch IE, Sze P. Visual experience during cataract surgery. Eye 1994;8:666–667.
2. Newman DK. Visual experience during phacoemulsification cataract surgery under topical anesthesia. Br J Ophthalmol 2000;84:13–15.
3. Au Eong KG, Lim TH, Lee HM, Yong VS. Subjective visual experience during phacoemulsification and intraocular lens implantation using retrobulbar anesthesia. J Cataract Refract Surg 2000;26:842–846.
4. Au Eong KG, Low CH, Heng WJ, et al. Subjective visual experience during phacoemulsification and intraocular lens implantation under topical anesthesia. Ophthalmology 2000;107:248–250.
5. Verma D. Subjective visual experience during phacoemulsification and intraocular lens implantation under topical anesthesia. Ophthalmology 2001;108:1004–1005.
6. Khan AO. Visual sensation in cataract surgery. Ophthalmology 2001;108:2157–2158.
7. Chung CF, Lai JS, Lam DS. Visual sensation during phacoemulsification and intraocular lens implantation using topical and regional anesthesia. J Cataract Refract Surg 2004;30:444–448.
8. Rengaraj V, Radhakrishnan M, Eong KG, et al. Visual experience during phacoemulsification under topical versus

retrobulbar anesthesia: results of a prospective, randomized, controlled trial. Am J Ophthalmol 2004;138:782–787.
9. Tan CS, Eong KG, Kumar CM. Visual experiences during cataract surgery: what anesthesia providers should know. Eur J Anesthesiol 2005;22:413–419.
10. Tan CS, Mahmood U, O'Brien PD, et al. Visual experiences during vitreous surgery under regional anesthesia: a Multicenter Study. Am J Ophthalmol 2005;140:971–975.
11. Mandelcorn MS, Mandelcorn E, Ananthanarayan C, Fleming JM. Some observations concerning visual perception during vitrectomy after retrobulbar anesthesia. Can J Ophthalmol 1997;32:255–256.
12. Sugisaka E, Shinoda K, Ishida S, et al. Visual sensations during vitrectomy. Ophthalmology 2006;113:1886. e1–e2.
13. Kawaguchi N, Inoue M, Sugisaka E, et al. Subjective visual sensation during vitrectomy under retrobulbar anesthesia [letter]. Am J Ophthalmol 2006;141:407–409.
14. Levin ML, O'Connor PS. Visual acuity after retrobulbar anesthesia. Ann Ophthalmol 1989;21:337–339.
15. Brent BD, Singh H. The effect of retrobulbar anesthesia on visual acuity in planned extracapsular cataract extraction. Ophthalmic Surg 1991;22:392–395.
16. Schimek F, Steuhl KP, Fahle M. Retrobulbar blockade of somatic, motor, and visual nerves by local anesthetics. Ophthalmic Surg 1993;24:171–180.
17. Westheimer G. Entoptic phenomena. In: Kaufman PL, Alm A, eds. Adler's physiology of the eye. St Louis, Missouri: Mosby Inc, 2003:441–452.

AJO History of Ophthalmology Series

Truman's Hyperopia

Can glasses change the course of history? Harry S. Truman was a high hyperope with an adult refraction showing a spherical equivalent of about +6 D. His hyperopia and blurry vision was discovered at the age of five. A child with glasses in rural Missouri in the late 19th Century was very unusual. He gravitated toward books and piano and stayed away from sports. He originally applied to West Point in 1901, but was rejected because of his ametropia. When the US entered World War I in 1917, he was accepted as an artillery officer in the Missouri National Guard. Would he have entered politics if he had become a career Army Officer? It is one of the 'What If's' of American History.

Provided by Darron A. Bacal, MD, of the Cogan Ophthalmic History Society.

Assessment of the posterior segment of the cat eye by optical coherence tomography (OCT)

Florian Gekeler,* Helmut Gmeiner,* Michael Völker,* Helmut Sachs,* Andre Messias,* Corinna Eule,† Karl Ulrich Bartz-Schmidt,* Eberhart Zrenner* and Kei Shinoda*

*University Eye Hospital, Schleichstrasse 12-16, D-72076 Tübingen, Germany; †Small Animal Clinic, Free University, Oertzenweg 19B, 14163 Berlin, Germany

Address communications to:
Florian Gekeler
Tel.: +49 7071 2984786
Fax: +49 7071 295038
e-mail: gekeler@uni-tuebingen.de

Abstract

Objectives To assess the feasibility of optical coherence tomography (OCT) for examining the cat ocular fundus, to provide normative data on retinal thickness in different fundus regions, and to demonstrate selected surgically induced vitreoretinal pathologies in the cat.

Animal studied Forty-five eyes of 28 healthy domestic cats and two eyes of domestic cats that had undergone subretinal implantation surgery for a visual prosthesis were examined.

Procedures An optical coherence tomograph (Zeiss-Humphrey) was used to examine the anesthetized animals. At least five vertical and five horizontal scans in regular distribution were recorded for each cat including (1) the peripapillary region, (2) the area centralis, and (3) the peripheral retina. Thickness was measured manually at five locations in each scan. Retinal thickness was compared in the three above-mentioned fundus regions, between eyes and between vertical and horizontal scans. OCT was additionally performed in animals with retinal detachment and a subretinal visual prosthesis.

Results OCT measurements required only minimal adjustments of human settings and yielded high quality images. In comparison to humans intraretinal layers were more difficult to differentiate. Retinal thickness was highest in the peripapillary region (245 ± 21 μm), followed by the peripheral retina (204 ± 11 μm) and the area centralis (182 ± 11 μm; all $P < 0.0001$). There was no statistically significant difference between right and left eye or between vertical and horizontal scans. OCT demonstrated retinal detachment, an iatrogenic break and a subretinal prosthetic device in high detail.

Conclusions Retinal thickness was measurable with high precision; values compare well to older histologic studies. OCT bears significant advantages over histology in enabling one to repeat measurements in living animals and thus allowing longitudinal studies. Various vitreoretinal pathologies common in feline eyes are detectable and quantifiable by OCT.

Key Words: cat, detachment, OCT, optical coherence tomography, retina, thickness

INTRODUCTION

Optical coherence tomography (OCT) has proven to be an extremely valuable diagnostic tool in ophthalmology and currently has widespread application in humans.[1] It is a noncontact, noninvasive imaging technique that produces high-resolution images of various ocular structures.

OCT is often compared to B-scan ultrasonography. It relies, however, upon reflections of light instead of dynamic echoes of ultrasound to yield a two-dimensional image of the retina. Utilization of light provides OCT with very high spatial resolution (in the region of 10 μm) compared to conventional posterior-segment ultrasonography (approximately 150 μm).[2] OCT is based on the principle of coherence interferometry wherein an infrared (approximately 830 nm wavelength) beam created by a superluminescent diode source is projected from the OCT unit onto the retina in a scanning fashion.[1,3] The beam is focused on the retina by a convex lens. A second beam (internal reference beam) is projected at a known reference distance. When the two light beams (internal reference beam and the back-scattered and back-reflected light from the retina) attempt to recombine,

the reference beam must be altered in order to combine with the diagnostic beam. The amount the reference beam is altered compared to its baseline to match the probe signal (optical path length difference) results in a signal generation. The magnitude of the back-scattered and reflected light from the target tissue is demonstrated as a false-color image in two dimensions. Variations in the optical characteristics of tissue account for differential reflective intensities and the associated heterogeneous false-color image appearance. Software manipulation of the raw OCT image data can result in quantitative retinal thickness measurements. Images are stored on digital media to enable comparison of serial evaluations and for archiving purposes.

A very high correlation between OCT findings and histologic examinations has been shown,[4] and OCT in clinical practice helps to identify structures such as epiretinal membranes, vitreoretinal tractions, accumulation of fluid in the subretinal space or neurosensory detachments, retinal detachments, retinoschisis, and retinal edema.[1] It has also been successfully applied to detect changes in the integrity of the retinal structure itself, such as by measuring the nerve fiber layer thickness for monitoring patients suffering from open-angle glaucoma and measuring the thickness of the photoreceptor-layer in retinitis pigmentosa (RP).[5] Resolution of clinical OCT varies between 10–20 μm and much less than 10 μm, depending on the model.[5,6] OCT imaging has several distinct advantages over other techniques. Paramount is its ability to repeatedly measure retinal structures in high resolution *in vivo*, which makes it feasible for longitudinal repeated measurements. Quantification of findings is possible in order to observe clinical development. Moreover, OCT does not suffer from artifactual changes, which are inherent in histologic examinations.

Recently ocular tissues other than the posterior segment such as the cornea and the lens have also been examined[7] and new technology is available for hand-held devices.[8]

While the principal possibility of examining the cat retina by OCT has been demonstrated in subretinal prosthesis surgery,[9] the intention in this study was to investigate the cat eye's posterior segment by OCT in more detail and provide normative data of retinal thickness in cats *in vivo*. Furthermore, various pathologic findings demonstrated by OCT are described.

MATERIALS AND METHODS

Experiments were performed on 28 healthy adult domestic cats. Sixteen cats were taken from a local private animal clinic with written consent from their owners and 12 cats were included from a study in the ophthalmology department of the University of Tübingen, Germany. In these cats both eyes were examined. In the second group only one eye was examined because the other eye had been used for subretinal implant surgery. Eye color was brown to blue-green; all eyes had a tapetum lucidum. No blue eyes were examined and none of the cats had an albinotic fundus. Experiments

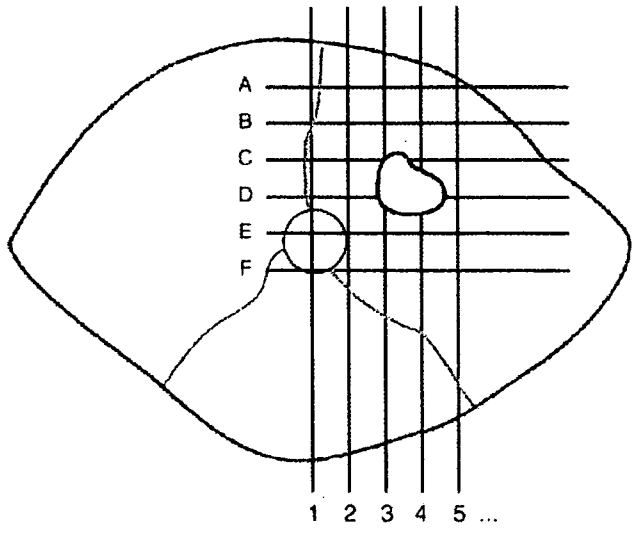

Figure 1. Diagram of the scan paths used (example shows a left eye with optic disk and area centralis). At least five vertical and horizontal scans were registered. Retinal thickness was measured manually in at least five locations along each scan path. Averages of retinal thickness were calculated for peripapillary and peripheral regions as well as thickness in the area centralis.

adhered to the Principles of Laboratory Animal Care (NIH publication no. 85–23, revised 1985), the OPRR Public Health Service Policy on the Humane Care and Use of Laboratory Animals (revised 1986) and the US Animal Welfare Act, as amended, as well as the local commission for animal welfare.

Anesthesia was achieved by intramuscular anesthesia of 15 mg/kg ketamine and 1 mg/kg xylazine. Inhalation narcosis was not applied for any cat. Pupils were dilated with atropine 1%. A lid retractor was used to keep the eyes open and corneas were moistened using standard artificial tears. Sometimes an indentator was used to align the eye with the machine's light beam by gentle pressure on the eyeball. Cats were placed in front of the optical coherence tomograph (Zeiss-Humphrey Inc., Dublin, CA, USA, software version A 6.1, 1997) on a cloth-covered table to ensure mechanical stability of the animal.

At least five horizontal and five vertical scans spaced approximately one optic disk diameter (ODD) starting inferior or nasal to the optic disk and extending over the area centralis towards the superior or temporal side were taken in all animals (Fig. 1). A digital video image was taken to visualize the OCT scan's position on the retina. In some animals ODD was assessed. Scan length was usually 4.3 mm (if not otherwise mentioned) and the eye length was adjusted to 21.50 mm in the set-up menu according to the manufacturer's recommendation and ultrasonic measurements of the feline eye.[10] Thickness and horizontal length measurements (in μm or mm, respectively) were performed using the instrument's built-in algorithm; accuracy of the automatic detection of the borders of the neurosensory retina was checked individually. If retinal borders were not detected correctly manual thickness

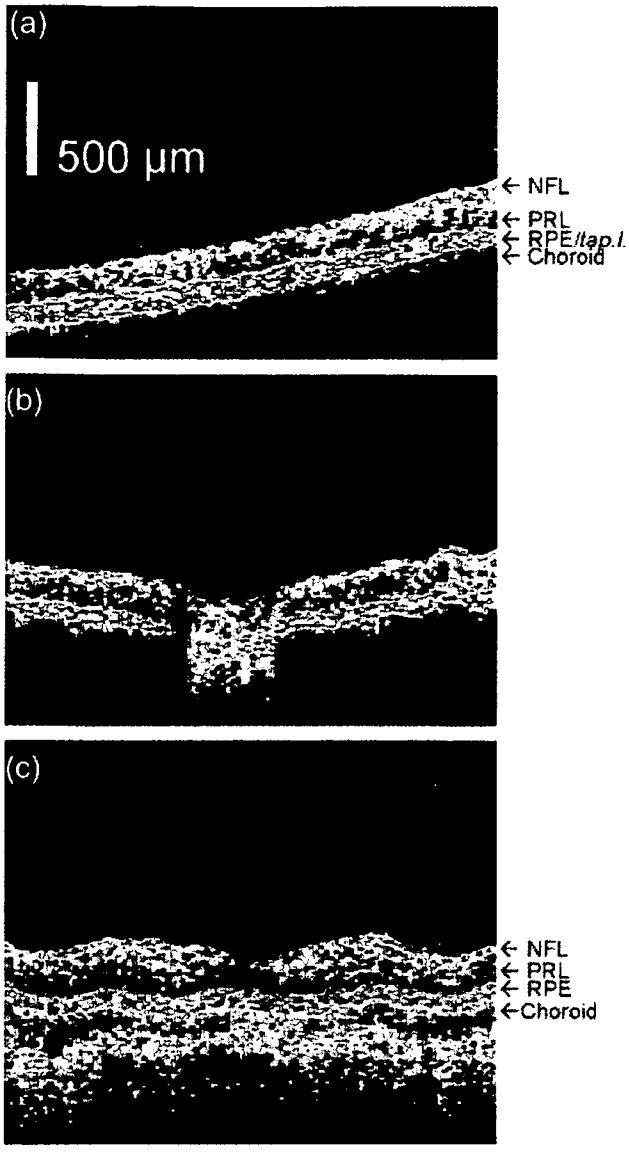

Figure 2. Representative OCT images of the cat retina and one example from a human retina for comparison (NFL, retina nerve fiber layer; PRL, photoreceptor layer; RPE, retina pigment epithelium; tap. l., tapetum lucidum). (a) Retinal OCT scan in the area centralis of one representative cat. The cat retina has a more homogeneous appearance than the human retina in OCT, which makes it more difficult to distinguish between different retinal layers. (b) Retinal OCT scan over the cat's optic disk. (c) Retinal OCT scan of a human eye showing the typical foveal depression of primate eyes. In human eyes more intraretinal layers are clearly observable.

measurement was performed using two arrows in the machine's algorithm.

All examinations and measurements were performed by an experienced clinician of the university eye hospital. Statistical analyzes were performed using paired *t*-test algorithms in STATISTICA® (version 5.5; StatSoft Inc., Tulsa, OK, USA).

Table 1. Retinal thickness as measured by OCT in micrometers in different regions of the posterior pole

Region	Peripapillary	Area centralis	Periphery
Average	245	182	204
Standard deviation	21	11	11
Minimum	209	162	179
Maximum	298	209	228

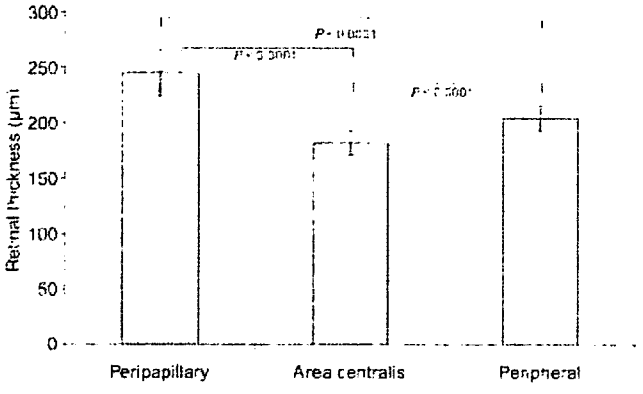

Figure 3. Retinal thickness as measured by OCT in different retinal areas of the cat. Average retinal thickness was different in the above-mentioned areas: it was highest near the optic disk, followed by the peripheral retina, and lowest in the area centralis. All comparisons showed highly significant differences.

RESULTS

It was possible to obtain high-quality OCT images in all cats in at least five vertical and five horizontal sections. In a few animals up to eight scans in vertical and horizontal direction were obtainable. However, at times extreme torsional eye movements of the animals inhibited examination of peripheral fundus areas. Because of the brightness of the highly reflective tapetum lucidum, ranges of the instrument had to be reduced to allow localization of the OCT beam on the video image. The OCT power and sensitivity had to be reduced by a factor of approximately 4. All other settings were comparable to human examinations. An advantage over clinical examination in patients was that animals were anesthesized and motion artifacts were thus usually minimal.

In general, the cat retina had a more homogenous appearance than the human retina, in which ideally the nerve fiber layer, the inner and outer plexiform layer, and the photoreceptor layer can be differentiated.[11] The subretinal layers in the cat showed a highly increased reflectivity and increased width compared to human eyes (Fig. 2a–c). In some eyes a narrow band of higher reflectivity on the vitreous side was identifiable (Fig. 2a).

The variance in retinal thickness was statistically significant across the posterior pole: it was highest in the peripapillary area, followed by the peripheral retina, and was lowest in the area centralis (Table 1, Fig. 3). Figure 4(a) demonstrates

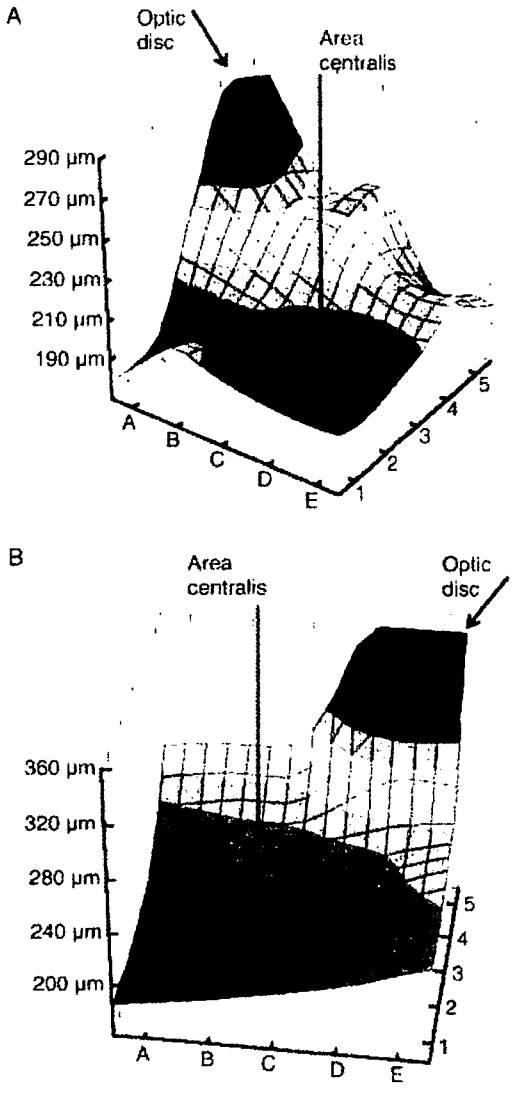

Figure 4. Surface plot of interpolated retinal thickness in two representative cats. Retinal thickness was measured at locations given in Fig. 1. Plots were rotated for better visibility of thickness distribution. (a) Right eye of one representative cat that demonstrated minimum thickness in the area centralis. (b) Left eye of one cat that did not show a typical clear minimum thickness in the area centralis.

a cat with a typical minimum retinal thickness in the area centralis, while Fig. 4(b) demonstrates one without this typical minimum.

There were no statistically significant differences between right and left eyes, or between horizontal and vertical scans ($P > 0.05$; data not shown). No vitreal-retinal pathologies were found in the healthy nonoperated cats, and specifically no posterior vitreous detachment, vitreous opacities/floaters, or retinal changes such as epiretinal membranes or edema were detected.

However, several pathologies could be verified by OCT in the cats that had undergone subretinal prosthesis surgery: a retinal detachment (Fig. 5), an iatrogenic retinal break, a small amount of retinal edema, and localized neurosensory detachment over a subretinal implant (Fig. 6).

DISCUSSION

Despite several distinct differences between cat and human eyes OCT assessment of the cat posterior pole was possible with only minor adjustments of the human settings. The differences, such as different eye size, the presence of a highly reflective tapetum lucidum in the cat and different pigmentation of the fundus did not play a significant role in the process of image gathering. The quality of the images was even somewhat higher in these animals because narcosis prevented practically all movements and thus virtually abolished motion artifacts which are common in human practice, often reducing image quality and prolonging examination times (Fig. 2).

The cat retina demonstrated a more homogeneous appearance than the human retina such that different intraretinal layers could hardly be identified. The narrow band of higher reflectivity on the vitreous side (see Fig. 2a,b) presumably corresponds to the posterior vitreous cortex or the internal limiting membrane of the retina. The broader band under the retina most probably corresponds to the complex of the tapetum lucidum and retinal pigment epithelium, which are both well expressed in feline eyes.[12] No clear photoreceptor layer was identifiable in our series as in humans. It is unclear whether different reflecting properties of the retina or the posterior pole in general played a role or whether these differences truly reflect anatomic differences.

Retinal thickness measurement was possible with high accuracy and high repeatability as demonstrated by high correspondence of values between vertical and horizontal scans as well as between right and left eye. As was to be expected retinal thickness varied across different regions of the cat's posterior pole. It was highest in the peripapillary region where ganglion-cell fibers concentrate to form the optic nerve. The area centralis showed the lowest thickness. Intermediate values were found in the peripheral retina. These thickness measurements compare well with values found in the literature: 195 µm in the peripheral retina (our study: 204 µm), and 150–220 µm in the area centralis (our study: 182 µm).[13] While histology allows thickness measurements with higher precision than OCT, histology suffers from inherent limitations of artifactual changes from the necessity of preparation and embedding of the material.

In the second group, which had undergone subretinal prosthesis surgery, we demonstrated the capability of OCT to detect retinal detachment, a small retinal break, a neurosensory detachment and the subretinal prosthetic device. Therefore, it seems to be well within the reach of this technique to detect, prove or disprove and, moreover, quantify a number of retinal diseases that have been described in cats. Retinal detachment is one of these (e.g. in infectious diseases such as FIV, toxoplasmosis, mycoses, tuberculosis): retinal degeneration is another and has been described in cats as hereditary

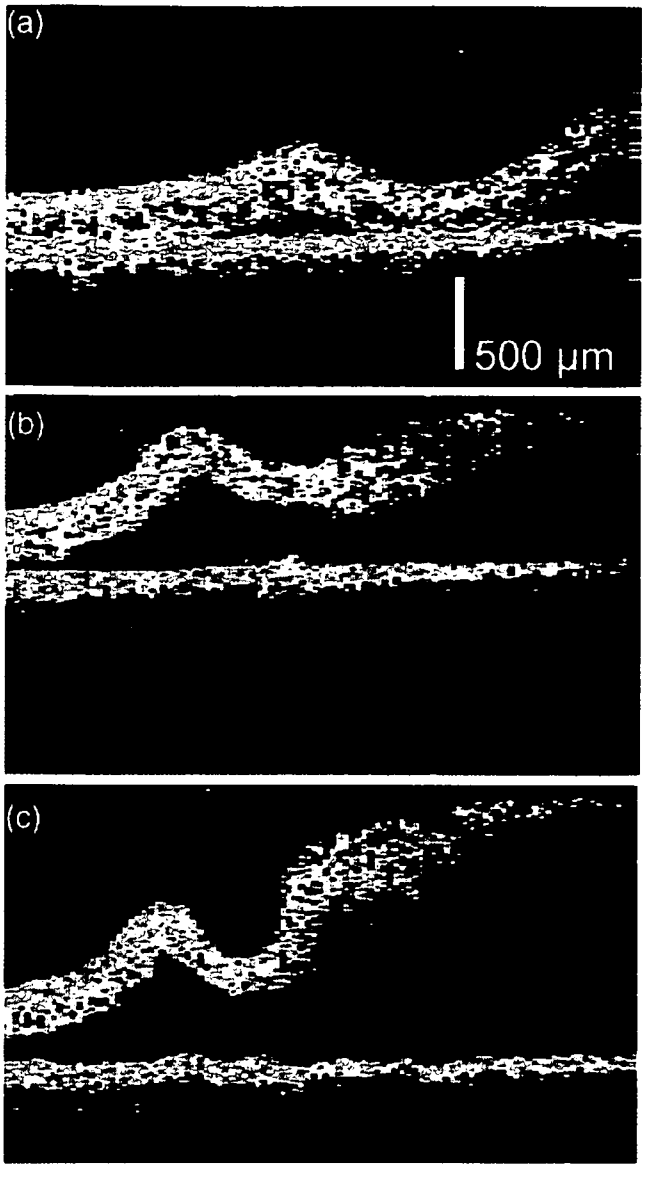

Figure 5. OCT scans of a cat that suffered from retinal detachment after retinal implant surgery. (a) Retinal OCT scan showing the beginning of retinal detachment on the posterior pole. (b) Retinal OCT scan showing progression of retinal detachment as the scan moves more peripheral. (c) Retinal OCT scan showing the maximum extent of retinal detachment.

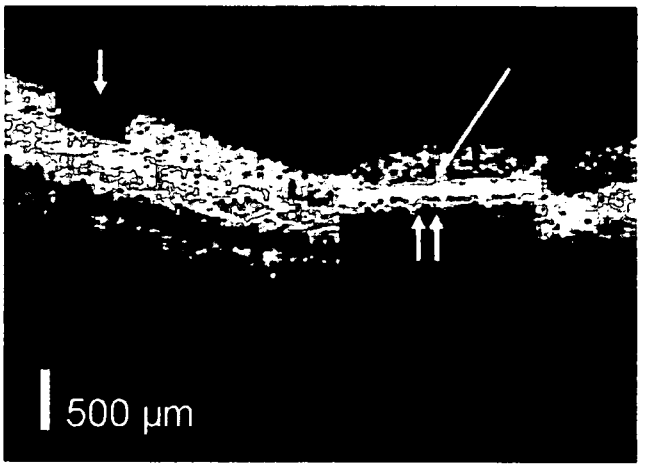

Figure 6. OCT scan showing a subretinal implant and an iatrogenic retinal break. The picture was acquired in an animal that underwent subretinal implant surgery 1 day earlier. The OCT scan demonstrates an iatrogenic retinal break on the left (short arrow), which was performed to introduce the device into the subretinal space. On the right the subretinal device is seen as a white (highly reflective band; double arrow). The retina over this device is somewhat elevated with subretinal fluid accumulation, possibly remnants of the viscoelastic material used during surgery (long, thin arrow). Scan length was 6.5 mm for this image. The iatrogenic break was measured at 0.5 mm; the diameter of the subretinal device was accurately measured at 2 mm.

rod-cone dysplasia[14] and in certain alimentary conditions such as taurine deficiency.[15] In humans retinal degeneration such as retinitis pigmentosa leads to retinal atrophy with retinal thinning, which has been successfully quantified by OCT.[16] Also, certain drugs can lead to retinal atrophy (e.g. the antibiotic enrofloxacin) in a range that is measurable by OCT.[17] Other diseases where OCT can aid in establishing the diagnosis or following the clinical course include retinal hemorrhage, optic nerve coloboma, optic nerve hypoplasia, optic neuritis with consecutive optic nerve head swelling (see Fig. 2b for a normal optic nerve configuration), progressive retina atrophy in the cat, true retinitis or choroiditis, hypertensive retinopathy, retinal and choroidal tumors, and intraocular or intraretinal foreign bodies.[12]

For this study we had access to an OCT of a (now) previous generation. Currently the Stratus® optical coherence tomograph model 3000 (Carl Zeiss Meditec AG, Jena, Germany) yields more detailed pictures with a resolution of less than 10 µm in comparison to the estimated 10–20 µm resolution of the machine used in our study.[6] For determining retinal thickness and discovering different retinal pathologies (such as small neurosensory detachments, retinal edema, retinal breaks, and retinal detachment), which were the main objectives of our study, a resolution of 10 to 20 µm is by far sufficient. It can be expected, however, that a higher resolution will give more insight into intraretinal anatomic structure than the previous generation. The increase in use of Stratus® OCT in general might lead to this more advanced technique being available for animal use in the future. However, pricing is much higher and availability of the previous OCT generation is greater worldwide; it therefore seems probable that it will currently be more easily accessible for veterinary use.

OCT will presumably not become a standard diagnostic tool for veterinary ophthalmologists in the near future. However, rising demands of the rapidly expanding field of veterinary ophthalmology go hand in hand with a necessity to diagnose and quantify more and more vitreoretinal pathologies. Decreasing prices of machines and associations

that are often possible with an institution that provides these facilities for humans could additionally help to increase the use of OCT. Moreover, the cat is arguably the best studied animal in vision research and exact diagnosis is mandatory under many circumstances in laboratory animals such as in prosthesis surgery, toxicity testing, and experimentally induced retinal pathologies. OCT allows exact diagnosis in many cases where this is not possible by other techniques. It allows quantification of findings and, because it is an *in vivo* noninvasive technique, it allows repeated measurements in clinical observation for longitudinal studies.

In conclusion, our study provides proof of the feasibility of using OCT in cat eyes. As the dog's posterior pole is extremely similar with regards to retinal structure and posterior ocular layers,[12] it is reasonable to expect similar possibilities with OCT in this species as well. We have acquired normative *in vivo* data of retinal thickness in different areas of the cat fundus demonstrating relative thinning in the area centralis. By demonstrating the capabilities of the technique in various vitreoretinal diseases in cats we believe that OCT can be of value in diagnosing and following clinical courses in a large number of other diseases typical for the feline eye. OCT bears significant advantages over other techniques by allowing high-resolution, quantifiable *in vivo* imaging, making it available for longitudinal studies.

REFERENCES

1. Thomas D, Duguid G. Optical coherence tomography - a review of the principles and contemporary uses in retinal investigation. *Eye* 2004; **18**: 561–570.
2. Mosfeghi VA, Mavrofrides AD, Puliafito CA. Optical coherence tomography and retinal thickness assessment for diagnosis and management. In: *Retina*. (ed. Ryan SJ) Mosby, Philadelphia, 2006; 1533–1556.
3. Huang Y, Cideciyan AV, Aleman TS *et al.* Optical coherence tomography (OCT) abnormalities in rhodopsin mutant transgenic swine with retinal degeneration (Letter). *Experimental Eye Research* 2000; **70**: 247–251.
4. Huang D, Swanson EA, Lin CP *et al.* Optical coherence tomography. *Science* 1991; **254**: 1178–1181.
5. Grieve K, Paques M, Dubois A *et al.* Ocular tissue imaging using ultrahigh-resolution, full-field optical coherence tomography. *Investigative Ophthalmology and Visual Science* 2004; **45**: 4126–4131.
6. Bourne RR, Medeiros FA, Bowd C *et al.* Comparability of retinal nerve fiber layer thickness measurements of optical coherence tomography instruments. *Investigative Ophthalmology and Visual Science* 2005; **46**: 1280–1285.
7. Fishman GR, Pons ME, Seedor JA *et al.* Assessment of central corneal thickness using optical coherence tomography. *Journal of Cataract and Refractive Surgery* 2005; **31**: 707–711.
8. Salmon JH, Buckland E, Woo S *et al.* Retinal imaging of the dog and rabbit using a hand-held, high resolution, optical coherence tomography system (Abstract). *Investigative Ophthalmology and Visual Science* 2006; **47**: 3311.
9. Volker M, Shinoda K, Sachs H *et al.* In vivo assessment of subretinally implanted microphotodiode arrays in cats by optical coherence tomography and fluorescein angiography. *Graefe's Archives for Clinical and Experimental Ophthalmology* 2004; **242**: 792–799.
10. Gilger BC, Davidson MG, Howard PB. Keratometry, ultrasonic biometry, and prediction of intraocular lens power in the feline eye. *American Journal of Veterinary Research* 1998; **59**: 131–134.
11. Puliafito CA, Hee MR, Lin CP *et al.* Imaging of macular diseases with optical coherence tomography. *Ophthalmology* 1995; **102**: 217–229.
12. Martin CL. Vitreous and ocular fundus. In: *Ophthalmic Disease in Veterinary Medicine*. (ed. Martin CL) Manson Publishing, London, 2005; 401–470.
13. Buttery RG, Hinrichsen CF, Weller WL *et al.* How thick should a retina be? A comparative study of mammalian species with and without intraretinal vasculature. *Vision Research* 1991; **31**: 169–187.
14. Leon A, Curtis R. Autosomal dominant rod-cone dysplasia in the Rdy cat. 1. Light and electron microscopic findings. *Experimental Eye Research* 1990; **51**: 361–381.
15. Aguirre GD. Retinal degeneration associated with the feeding of dog foods to cats. *Journal of the American Veterinary Medical Association* 1978; **172**: 791–796.
16. Sandberg MA, Brockhurst RJ, Gaudio AR *et al.* The association between visual acuity and central retinal thickness in retinitis pigmentosa. *Investigative Ophthalmology and Visual Science* 2005; **46**: 3349–3354.
17. Wiebe V, Hamilton P. Fluoroquinolone-induced retinal degeneration in cats. *Journal of the American Veterinary Medical Association* 2002; **221**: 1568–1571.

the evaluation for CTX to support early definitive therapy. Moreover, the measurement of cholestanol levels when a subject is initially seen with presenile cataracts of questionable etiology could be a valuable clinical tool.

Alexandra Tessás, MD
Zoltán Pfund, MD
Éva Morava, MD, PhD
György Kosztolányi, MD, DSci
Erik Sistermans
Ron A. Wevers
Richard Kellermayer, MD, PhD

Correspondence: Dr Kellermayer, Department of Medical Genetics and Child Development, University of Pecs, József A u. 7., Pécs 7623, Hungary (richard.kellermayer@aok.pte.hu).

Financial Disclosure: None reported.

1. Forsius H, Arentz-Gustvedt E, Eriksson AW. Juvenile cataract with autosomal recessive inheritance: a study from the Aland Islands, Finland. *Acta Ophthalmol (Copenh)*. 1992;70:26-32.
2. Verrips A, van Engelen BG, Wevers RA, et al. Presence of diarrhea and absence of tendon xanthomas in patients with cerebrotendinous xanthomatosis. *Arch Neurol*. 2000;57:520-524.
3. Lorincz MT, Rainier S, Thomas D, Fink JK. Cerebrotendinous xanthomatosis: possible higher prevalence than previously recognized. *Arch Neurol*. 2005;62:1459-1463.
4. Batta AK, Salen G, Tint GS. Hydrophilic 7 beta-hydroxy bile acids, lovastatin, and cholestyramine are ineffective in the treatment of cerebrotendinous xanthomatosis. *Metabolism*. 2004;53:556-562.
5. van Heijst AF, Verrips A, Wevers RA, Cruysberg JR, Renier WO, Folboom JJ. Treatment and follow-up of children with cerebrotendinous xanthomatosis. *Eur J Pediatr*. 1995;154:513-516.

Familial Retinal Arterial Tortuosity Associated With Tortuosity in Nail Bed Capillaries

Familial retinal arterial tortuosity (FRAT) is characterized by marked tortuosity of second- and third-order retinal arteries with normal first-order arteries and venous system. Patients have variable transient vision loss owing to retinal hemorrhages after minor stress or trauma. Prognosis is usually excellent. Whether there is systemic involvement is controversial. We report 3 cases of FRAT associated with a high degree of tortuosity of capillaries at nailfold capillaroscopy as an indication of systemic vascular pathology.

Report of Cases. *Case 1.* A woman was first seen at age 19 years because of blurred vision after a minor car accident. Best-corrected visual acuity (BCVA) was 0.9 OD and 0.8 OS. Ophthalmologic examination revealed marked tortuosity of second- and third-order retinal arteries and multiple intraretinal and preretinal hemorrhages in both eyes (**Figure 1**A). The patient was observed. Four weeks later, BCVA was fully restored in both eyes and the hemorrhages had almost resolved.

Five years later, the patient reported frequent episodes of migraine. Tortuosity of the retinal vessels and BCVA remained unchanged, but the macular reflex appeared duller, and mild thickening of the inner limiting membrane was noted in both eyes (Figure 1B). No hemorrhages were observed.

Seven years after she was first seen, the patient had decreased visual acuity of 0.4 OD and 0.8 OS. She was in her 18th week of pregnancy and had undergone amniocentesis 2 days previously. Fundus examination showed several preretinal, foveal hemorrhages in both eyes. Four weeks later, BCVA returned to 1.0 OU and hemorrhages had resolved.

Twelve years after she was first seen, the patient reported episodes of blurred vision once per year, usually following minor exercise. Best-corrected visual acuity had always fully recovered. At this ophthalmologic examination, thickening of the inner limiting membrane was stable and there was 1 asymptomatic preretinal hemorrhage inferotemporal to the macula (Figure 1C). The patient still experienced 5 to 6 episodes of migraine per year but was otherwise healthy.

In visual field tests, scotomas were noted that corresponded to the locations of the hemorrhages. Fluorescein angiography demonstrated no leakage, staining, hypoperfusion, or capillary dropout. Neurologic examinations, including cranial magnetic resonance imaging, yielded normal findings. Extensive examinations in internal medicine, explicitly, tests for serologic factors including virus and bacteria antibody titers and for rheumatologic and autoimmune factors, coagulation tests, and serum electrophoresis, also yielded normal findings. The patient was not taking any systemic medication that would alter coagulation, and blood pressure was within normal limits.

At nailfold capillaroscopy, which was performed at the second and fourth visits, tortuosity of capillaries was highly increased in all fingers of both hands (Figure 1D and E). Minor rarefication and 1 avascular zone, but no microhemorrhages, were detected. Sodium fluorescein video nailfold capillaroscopy showed normal inflow and outflow demonstrating absence of capillary spasm; normal transcapillary and interstitial diffusion of fluorescein; and normal halo. No other dermatologic disease, including Raynaud syndrome, was observed.

Case 2. The older sister of patient 1 reported a slight decrease in BCVA when first seen at age 28 years. However, BCVA was 1.0 OU. We found marked tortuosity of second- and third-order retinal arteries in both eyes but no hemorrhages. The patient had a history of 1 episode of transient microhematuria of unknown origin, but otherwise reported that she was healthy.

Seven years later, extensive ophthalmologic (**Figure 2**A), neurologic, and medical examinations were performed, analogous to those in patient 1. All findings were normal with the exception that antinuclear antibodies were 2-fold positive. Findings at dermatologic examination and nailfold capillaroscopy were identical to those in patient 1 (Figure 2B and C).

Case 3. The father of patients 1 and 2 was first seen at age 56 years and reported that he had never experienced any visual disturbances. He had a stroke with speech disturbance 8 years earlier, but reported no residual adverse effects. Best-corrected visual acuity was 1.0 OU. Marked tortuosity of second- and third-order retinal arteries was found in both eyes, without hemorrhages.

He was seen 7 years later, and extensive ophthalmologic (**Figure 3**A), neurologic, and medical examinations revealed atrial fibrillation, and

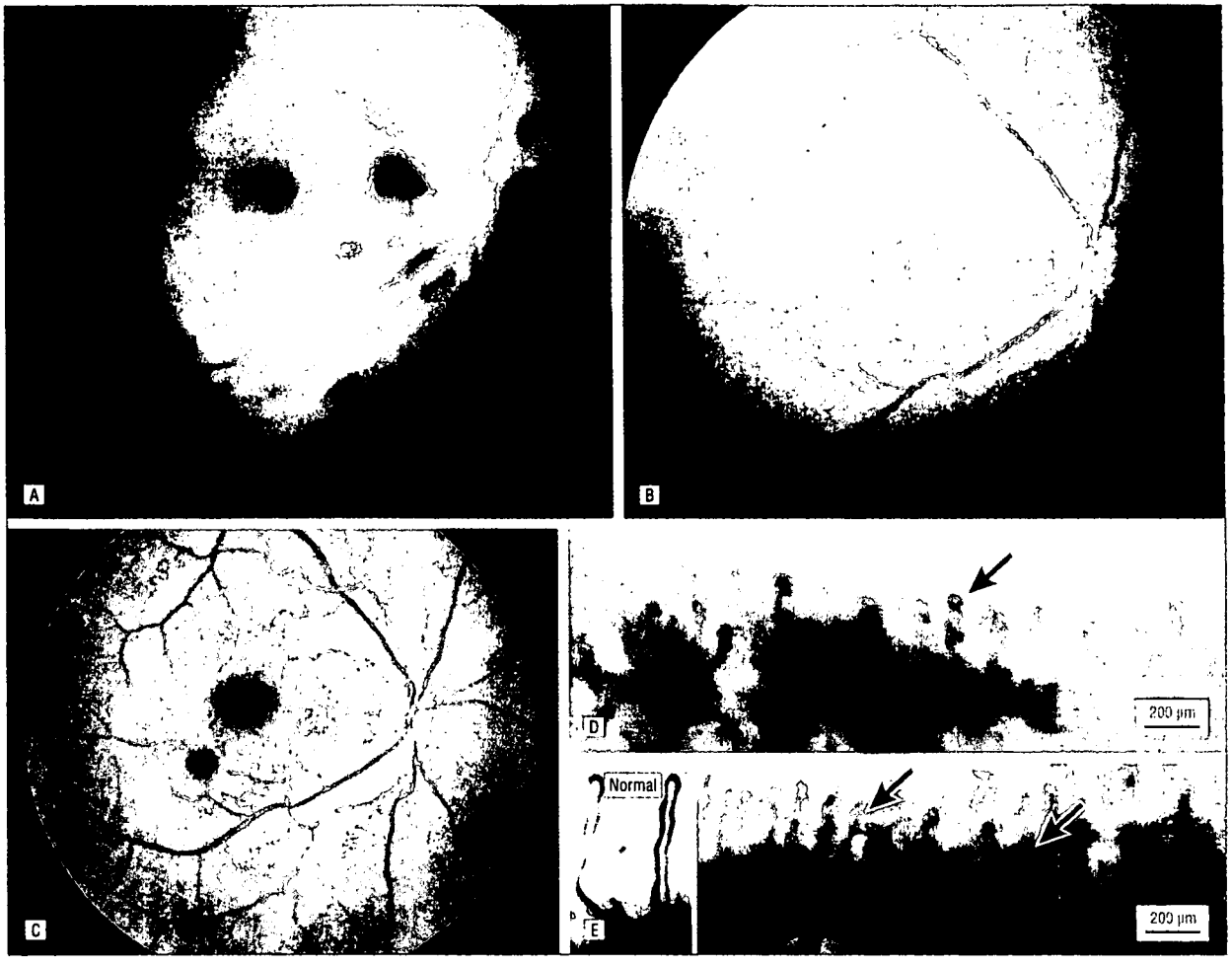

Figure 1. Patient 1. Views of the fundus and findings at nailfold capillaroscopy. A, When the patient was first seen after a minor car accident at age 19 years, multiple small hemorrhages were noted. She exhibited all of the typical features of familial retinal arterial tortuosity, with tortuosity in second- and third-order retinal arteries and normal large arteries and retinal veins. B, Five years later, no hemorrhages were seen and the retinal vasculature remained unchanged. C, Twelve years later, there was 1 preretinal hemorrhage inferotemporal to the macula; the retinal vasculature otherwise remained unchanged. D and E, Nailfold capillaroscopic findings in the right third and fourth fingers. Except for the high degree of tortuosity (present in approximately 30% of capillary loops; arrows depict typical examples), the capillaries were normal, a finding that was confirmed at sodium fluorescein video microscopy. For comparison, the inset in E shows enlargement of normal capillary loops at nailfold capillaroscopy in a healthy person. Note parallel arrangement of inflow and outflow arms.

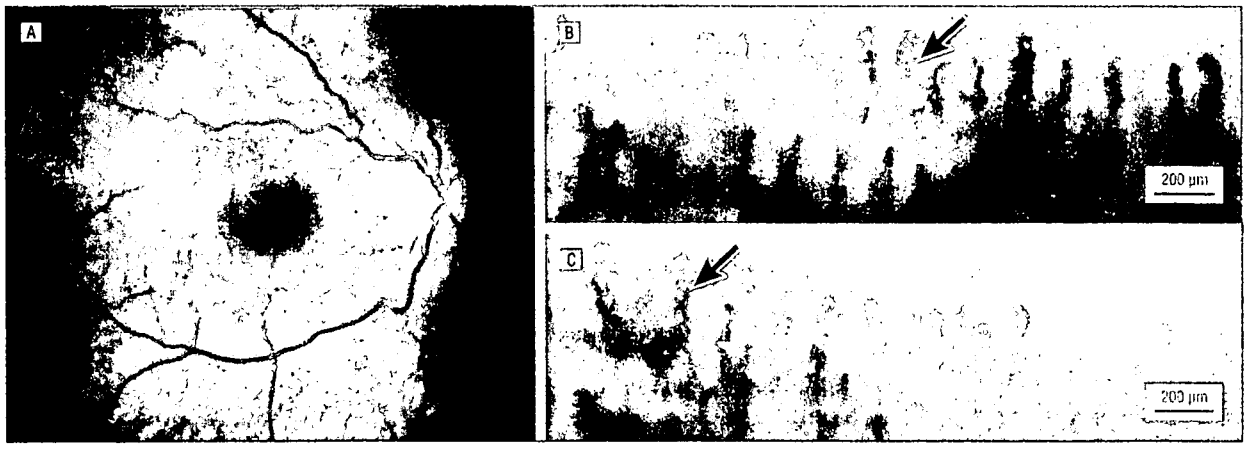

Figure 2. Patient 2. Views of the fundus and findings at nailfold capillaroscopy. A, At age 35 years, the patient demonstrated all of the typical findings of familial retinal arterial tortuosity. She had never experienced visual disturbances, although the degree of tortuosity was higher than in patient 1. B and C, Nailfold capillaroscopic findings in the left third and fourth fingers. Also in this patient, approximately 30% of capillary loops showed a high degree of tortuosity (arrows depict typical examples), while all other findings were normal, analogous to those in patient 1.

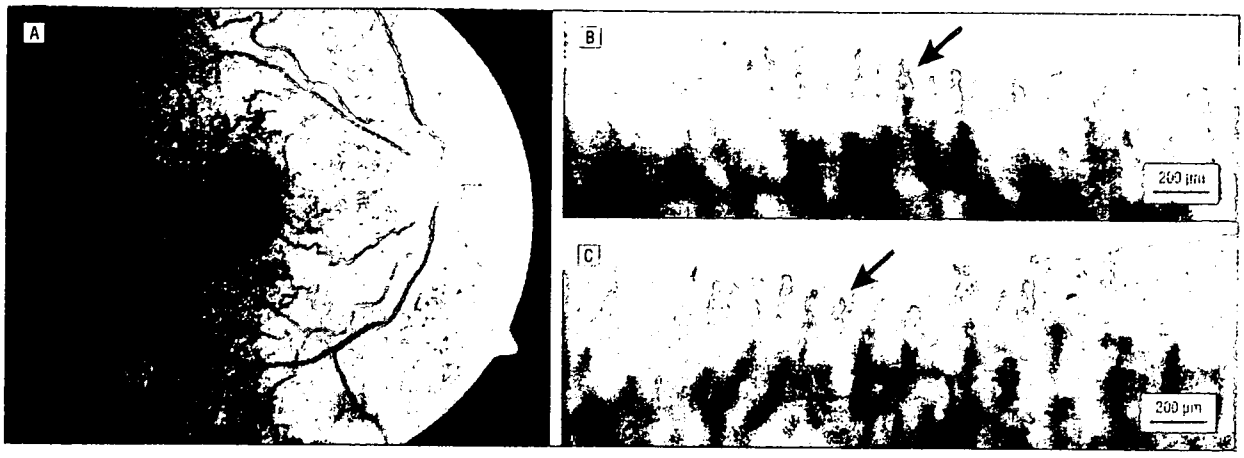

Figure 3. Patient 3. Views of the fundus and findings at nailfold capillaroscopy. A, When the patient was last seen at age 62 years, he demonstrated all of the typical findings of familial retinal arterial tortuosity. The patient had never experienced visual disturbances, although the degree of tortuosity was greater than in patients 1 and 2. B and C, Nailfold capillaroscopic findings in the patient's right second and fourth fingers. Approximately 30% of capillary loops showed a high degree of tortuosity (arrows depict typical examples), while all other findings were normal, analogous to those in patients 1 and 2.

warfarin sodium therapy was prescribed. As in patients 1 and 2, all other systemic findings were normal. Findngs at dermatologic examination and nailfold capillaroscopy were identical to those in patient 1 (Figure 2B and C).

Comment. All 3 patients had typical features of fRAT: only second- and third-order arteries were affected, while first-order arteries and the venous system were normal. The caliber, shape, and branchings of affected arteries were normal; no leakage or staining was observed at fluorescein angiography; symptomatic hemorrhages followed minor stress or trauma; visual prognosis was excellent; and no associated systemic disease was found in any of our 3 patients. These findings correspond well with the previously reported approximately 100 cases.[1,2] While in isolated cases systemic disease was found in patients with fRAT (malformation in the Kieselbach nasal septum, vascular mass in the spinal cord, sixth nerve palsy, simultaneous conjunctival hemorrhage, teleangiectasis of the bulbar conjunctiva), no consistent associated systemic disease has been reported and, thus, fRAT was generally believed to be an isolated retinal finding.[2,3] Our finding of marked capillary tortuosity at nailfold capillaroscopy favors systemic vascular disease in fRAT.

Recently, a syndrome has been reported consisting of features of fRAT with hematuria, muscular contractures, and sporadic other disorders such as cardiac arrhythmia.[4] This syndrome is distinct from the finding in our patients: only patient 2 had transient microhematuria and pronounced tortuosity in nail bed capillaries, in contrast to the unspecific findings at nailfold capillaroscopy found in patients with the newly reported syndrome, which is dominated by renal disease.

Nailfold capillaroscopy, as it was performed in our patients, is considered a mirror of systemic vascular processes, and a high degree of validity of correspondence and prognostic value is found, for example, in diabetes mellitus, systemic scleroderma, primary chronic polyarthritis, and systemic lupus erythematosus, and especially with ocular capillaries and in glaucoma.[5] Nailfold capillaroscopy demonstrated the identical features of capillary loops as retinal vessels in showing a high degree of tortuosity without any other pathologic findings such as leakage of dye, occlusion, or caliber abnormalities. A milder form of tortuosity at nailfold capillaroscopy has been described in patients with psoriatic arthritis,[6] but, to our knowledge, tortuosity of this magnitude has not been reported before. Considering that hemorrhages from retinal vessels are a hallmark of fRAT, manifestation in other tissues could be expected, although evidence for consistent systemic disease is thus far lacking in fRAT.

By demonstrating that capillary abnormalities are also found in nailfold capillaries of patients with fRAT, retinal vascular abnormalities can no longer be accepted as an isolated finding. We believe that, because of an increasing number of reports of this disease,[1] further investigation as to systemic involvement in patients with fRAT is warranted.

Florian Gekeler, MD
Kei Shinoda, MD, PhD
Michael Jünger, MD
Karl Ulrich Bartz-Schmidt, MD
Faik Gelisken, MD

Correspondence: Dr Gekeler, Department of Ophthalmology, University of Tübingen, Schleichstrasse 12-16, 72076 Tübingen, Germany (gekeler@uni-tuebingen.de).

Financial Disclosure: None reported.

Additional Information: This study conformed to the protocol of our institutional review board and did not require approval.

1. Gass DM. Macular dysfunction caused by retinal vascular diseases. In: Gass DM, ed. *Stereoscopic Atlas of Macular Diseases*. 4th ed. St Louis, Mo: Mosby-Year Book Inc; 1997.
2. Sutter FK, Helbig H. Familial retinal arteriolar tortuosity: a review. *Surv Ophthalmol*. 2003; 48:245-255.
3. Sears J, Gilman J, Sternberg P Jr. Inherited retinal arteriolar tortuosity with retinal hemorrhages. *Arch Ophthalmol*. 1998;116:1185-1188.
4. Plaisier E, Alamowitch S, Gribouval O, et al. Autosomal-dominant familial hematuria with retinal arteriolar tortuosity and contractures: a novel syndrome. *Kidney Int*. 2006;67:2351-2360.
5. Flammer J, Pache M, Resink T. Vasospasm: its role in the pathogenesis of diseases with particular reference to the eye. *Prog Retin Eye Res*. 2001;20:319-349.
6. Grassi W, Cervini C, Carline G, Cervini L. Nailfold capillary permeability in psoriatic arthritis. *Scand J Rheumatol*. 1992;21:226-230.

Clinical and Experimental Ophthalmology 2007; 35: 693–696
doi: 10.1111/j.1442-9071.2007.01580.x

Surgical Technique

Two-step oblique incision during 25-gauge vitrectomy reduces incidence of postoperative hypotony

Makoto Inoue MD,[1,2] Kei Shinoda MD,[1,3] Hajime Shinoda MD,[1] Ryosuke Kawamura MD,[1] Kotaro Suzuki MD[1] and Susumu Ishida MD[1]

[1]Department of Ophthalmology, Keio University School of Medicine, [2]Kyorin Eye Center, Kyorin University School of Medicine, Tokyo, and [3]Department of Ophthalmology, Oita University School of Medicine, Oita, Japan

ABSTRACT

The efficacy of a two-step, oblique incision procedure during 25-gauge vitrectomy on postoperative hypotony was evaluated by a retrospective, case–control study. The transconjunctival incision during 25-gauge vitrectomy was made in two steps: penetration with a microvitreoretinal blade followed by a penetrater instrument of a blunt trocar. The two-step procedure was performed on 89 eyes and with the conventional incision on 68 eyes. The incidence of hypotony (intraocular pressure <6 mmHg) on the first postoperative day and after 1 week and 1 month was compared. Hypotony was found in two eyes (2%) with the two-step method and 12 eyes (18%) with the conventional incision on the first postoperative day ($P=0.001$, Fisher's exact probability test). The preoperative intraocular pressure was not significantly different in the two groups but was significantly higher in the two-step group than in the conventional method group on the first postoperative day ($P=0.001$, Wilcoxon rank test). Twenty-five-gauge vitrectomy with two-step oblique incisions will reduce the incidence of postoperative hypotony on the first postoperative day.

Key words: hypotony, oblique incision, 25-gauge vitrectomy, two-step.

INTRODUCTION

The use of 25-gauge instruments for vitrectomy[1] enables transconjunctival sutureless vitrectomy.[2–4] However, postoperative hypotony and choroidal detachment have been reported as postoperative complications.[5,6] To prevent postoperative hypotony, peripheral vitrectomy was not recommended to perform so that it can be incarcerated into the sclerotomy to reduce leakage.[2,4] However, the use of 25-gauge vitrectomy for other diseases that require peripheral vitrectomy increased the incidence of postoperative hypotony, endophthalmitis and expulsive haemorrhage although the hypotony and choroidal detachment usually recovered without additional treatment.[5,7]

Oblique sclerotomy and the scleral tunnel incisions using the conventional trocar-cannula were reported to minimize the incidence of wound leakage.[8,9] However, we hypothesized that a slit-shaped incision made by a microvitreoretinal (MVR) blade would enhance the postoperative sutureless wound closure.[10,11] Thus, we modified the technique of creating a sclerotomy for the 25-gauge vitrectomy termed a two-step, oblique incision method with a MVR blade followed by the penetrater instrument of a blunt trocar. The incidence of hypotony following this two-step procedure was determined retrospectively.

MATERIALS AND METHODS

The 25-gauge vitrectomy was performed on 157 eyes during 2005 and 2006 at the Keio University Hospital, Tokyo, and the follow-up period was at least 3 months. The two-step, oblique incision procedure during 25-gauge vitrectomy was performed on 89 eyes (oblique group) and compared with 68 eyes (conventional group) with 25-gauge vitrectomy using the conventional incision with the same type of cannula (Alcon, Fort Worth, TX, USA) that penetrated vertically. The surgical procedures were performed by a single surgeon (MI) and these cases were two overlapping consecutive series as the oblique incision technique was being developed. The procedures conformed to the tenets of the Declaration of Helsinki, and an informed consent was obtained from each individual after an explanation of the procedures.

The initial incision of two-step oblique incision was made with a MVR blade (25-gauge, Mani Corp, Utsunomiya, Japan), and the second step involved inserting a blunt trocar

■ *Correspondence* Dr Makoto Inoue, Department of Ophthalmology, Keio University School of Medicine, 35 Shinanomachi, Shinjuku-ku, Tokyo 160-8582, Japan. Email: inoshin@sc.itc.keio.ac.jp

Received 5 May 2007, accepted 5 July 2007

to guide the 25-gauge cannula (Alcon, Fort Worth, TX, USA). The tip of the trocar was modified to be round so that it easily penetrated the initial incision created by the MVR blade (Fig. 1). The width of the MVR blade was 0.52 mm, which was slightly smaller than the 0.54 mm diameter of the 25-gauge cannula. Before making the incision with the MVR blade, the conjunctiva at the site of the sclerotomy was moved circumferentially to displace the conjunctiva from the sclerotomy and held in place by the pressure plate (DORC International, Zuidland, the Netherlands), a part of the 23-gauge instruments to identify the sclerotomy site. The sclera was perforated by the MVR blade tangentially at an angle of 45°–60°, and parallel to the corneal limbus (Fig. 2a). The blunt trocar with the cannula was then inserted at the same angle through the incision with the aid of the pressure plate. When the tip of the trocar was inserted, its direction was altered by gently rotating the trocar to point towards the centre of the globe (Fig. 2b).

The vitreous surgeries in both groups included core vitrectomy, membrane peeling, membrane delamination and endophotocoagulation. The peripheral vitreous was removed up to the ora serrata with scleral indentation in all eyes including eyes with previous vitreous surgeries. Eyes with combined scleral buckling and silicon oil injection were excluded. The intraocular pressure (IOP) was kept at approximately 30 mmHg controlled by the height of the infusion bottle when the cannulas were removed at the end of the surgery. A cotton swab was used to gently massage the entry site to close the opening after the cannula was removed, and the IOP was adjusted by injecting balanced salt solution (BSS) plus/or gas into the anterior chamber or vitreous cavity.

The incidence of hypotony was defined as an IOP < 6 mmHg on the first postoperative day, and the values of preoperative IOP and postoperative IOP at 1 week and 1 month were compared between the two groups. IOP was measured with a Goldman aplanation tonometer. The patients whose preoperative IOP was <6 mmHg were excluded. The statistical analysis was performed by Wilcoxon rank test and Fisher's exact probability test to compare between the two groups.

Results

The age, gender ratio, operating time and the disease necessitating the operation are shown in Table 1. The mean age in the two groups ($P = 0.116$, Wilcoxon rank test), the gender ratio ($P = 0.520$, Fisher's exact probability test), the incidence of combined cataract surgery ($P = 0.076$, Fisher's exact probability test), history of previous vitreous surgery ($P = 0.502$, Fisher's exact probability test) and operating time ($P = 0.455$, Wilcoxon rank test) were not significantly different between the two groups. A gas tamponade was used in 28 eyes (31%) in the oblique group and 21 eyes (31%) in the conventional group ($P > 0.999$, Fisher's exact probability test). The preoperative IOP was 13.7 ± 2.6 mmHg in the oblique group and 12.9 ± 3.7 mmHg in the conventional group, and this difference was not significant ($P = 0.130$, Wilcoxon rank test).

The postoperative sclerotomies were slit-shaped in the oblique group and V-shaped in the conventional group (Fig. 3). A leakage of intraocular fluid from the sclerotomies or the wounds of cataract surgery was not observed in any

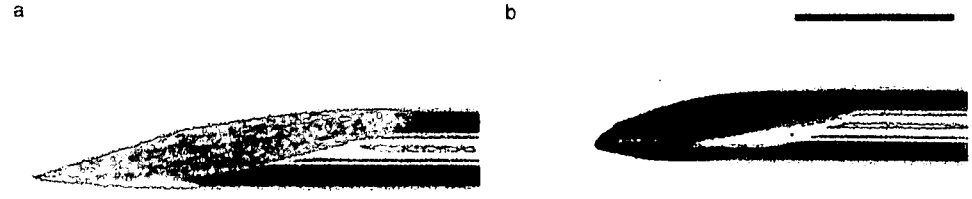

Figure 1. Microphotograph of the conventional and modified trocar. (a) The edge of the conventional 25-gauge trocar by Alcon. (b) The edge of the trocar is modified to be round from the same type of trocar of (a) (Bar: 1.0 mm).

Figure 2. Intraoperative photographs at the insertion of the trocar-cannula. (a) Initially, the microvitreoretinal blade penetrates the globe tangentially at an angle of 60° and parallel to corneal limbus. (b) Subsequently, the blunt trocar is inserted and the cannula is located at the sclerotomy.

eye in the two groups, but a shallow conjunctival bleb without leakage was occasionally seen in eyes with hypotony or some eyes with normal IOP. The mean IOP on the first postoperative day was significantly higher in the oblique group (14.3 ± 4.4 mmHg) than in the conventional group (10.0 ± 5.6 mmHg; $P = 0.001$, Wilcoxon rank test). After 1 week, the mean IOP was 14.4 ± 3.6 mmHg in the oblique group and 12.8 ± 5.4 mmHg in the conventional group ($P = 0.114$, Wilcoxon rank test); after 1 month, the mean IOP was 14.0 ± 2.3 mmHg in the oblique group and 14.6 ± 4.0 mmHg in the conventional group ($P = 0.220$, Wilcoxon rank test). None of the eyes with previous vitreous surgery developed postoperative hypotony.

A temporary hypotony or choroidal detachment was found in two of 89 eyes (2%) (Table 2) in the oblique group, and in 12 of 68 eyes (18%) in the conventional group ($P = 0.001$, Fisher's exact probability test). The IOP in all eyes with postoperative hypotony recovered to the preoperative IOP and the choroidal detachment disappeared within 2 or 3 days. In eyes without a gas tamponade, the incidence of postoperative hypotony on the first day was significantly lower ($P = 0.001$, Fisher's exact probability test) in the oblique group (1 of 61 eyes; 2%) compared with the conventional group (10 of 47 eyes; 21%). In eyes in which gas tamponade was used, however, the incidence of hypotony was not significant between the oblique group (1 of 28 eyes; 4%) and the conventional group (2 of 21 eyes; 10%, $P = 0.569$, Fisher's exact probability test). A postoperative retinal detachment developed in one eye in the conventional group because of the reopening of the original retinal break. The retina was reattached by additional endophotocoagulation and gas tamponade. None of the eyes developed a retinal break or retinal detachment related to the sclerotomies and peripheral residual vitreous.

Table 1. Preoperative conditions in the oblique and the conventional groups

	Oblique	Conventional	*P*-value
Number of eyes	89	68	
Age (year)			
Mean (SD)	64.4 (11.0)	59.3 (16.3)	0.116†
Gender (M/F)	49/40	41/27	0.520*
Preoperative IOP (mmHg)			
Mean (SD)	13.7 (2.6)	12.9 (3.7)	0.130†
Combined cataract surgery (eyes)	54	31	0.076*
Previous vitreous surgery (eyes)	4	5	0.502*
Gas tamponade (eyes)	28	21	>0.999*
Operating time			
Mean (SD)	49 (19)	55 (21)	0.455†

*Fisher's exact probability test; †Wilcoxon rank test. IOP, intraocular pressure; SD, standard deviation.

Discussion

The advantages of the 25-gauge vitrectomy system are faster postoperative recovery, lower invasiveness of surgery and a reduction of surgery-induced astigmatism. Kadonosono *et al.*[12] reported better visual acuity after 25-gauge vitrectomy than with the 20-gauge system at 1 month but not at 6 months for patients with an epiretinal membrane. Rizzo *et al.*[13] also reported a rapid visual improvement and less postoperative discomfort after 25-gauge vitrectomy for patients with an epiretinal membrane. In addition, the surgical times were shorter and less irrigating solution was used during the surgery.

It has, however, been shown that 25-gauge vitrectomy has some disadvantages such as the fragility of the thin instruments[14] and the temporary postoperative hypotony. The incidence of hypotony has been reported to be 8.5% (3/35 eyes) by Fujii *et al.*,[3] 0% (0/45 eyes) by Ibarra *et al.*[4] and 9% (15/162 eyes) by Shimada *et al.*[7] An oblique incision or a scleral tunnel technique has been suggested to be used to insert the conventional 25-gauge trocar-cannula tangentially at an angle of 30°–45° to avoid postoperative hypotony. Because the conventional needle-type trocar creates a

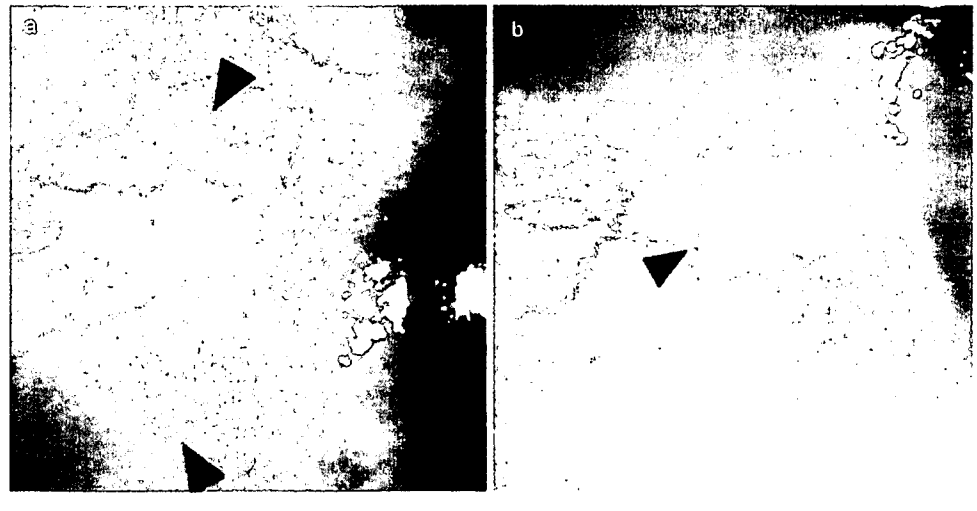

Figure 3. Photograph at the sclerotomy on the first postoperative day. (a) The sclerotomies of two-step incisions (arrow heads) that are slit-shaped without any bleb. (b) The sclerotomy of the conventional incision (arrow head) that is V-shaped.

Table 2. Comparison of the two-step oblique incision and the standard vertical incision

Surgical procedure	Total eyes with postoperative hypotony	Procedure (eyes) with postoperative hypotony	Number of eyes with disease
Two-step 25G oblique incision	2/89 (2%)*	No exchange: 1/61 (2%)** Gas exchange: 1/28 (4%)*** Cataract surgery: 1/54 (2%)**** Vitrectomy alone: 0/35 (0%)***** Previous vitrectomy: 0/4 (0%)******	Epiretinal membrane: 20 Macular hole: 17 RVO: 16 DME: 13 PDR: 12 Neovascular maculopathy: 6 Retinal detachment: 3 Uveitis: 2
Standard 25G vertical incision	12/68 (18%)	No exchange: 10/47 (21%)** Gas exchange: 2/21 (10%)*** Cataract surgery: 8/31 (26%)**** Vitrectomy alone: 2/37 (5%)***** Previous vitrectomy: 0/5 (0%)******	Epiretinal membrane: 21 Macular hole: 8 RVO: 5 DME: 11 PDR: 11 Neovascular maculopathy: 4 Retinal detachment: 4 Uveitis: 4

*$P = 0.001$, **$P = 0.001$, ***$P = 0.569$, ****$P = 0.001$, *****$P = 0.493$, ******$P > 0.999$ (Fisher's exact probability test). DME, diabetic macular oedema; 25G, 25-gauge; PDR, proliferative diabetic retinopathy; RVO, retinal vein occlusion.

V-shaped sclerotomy, the trocar should be inserted with the bevel-side down to obtain a water-tight sealing of the wound.[9] However, we hypothesized a slit-shaped incision would be a better shape incision to achieve a self-sealing wound.[10,11]

The two-step oblique method enabled us to achieve reliable wound construction during 25-gauge vitreous surgery and thus reduce the leakage of intraocular fluid and postoperative hypotony. The disadvantage of this method was the necessity of performing two steps instead of one step. Because of limited number of cases, further studies including randomized prospective study are necessary to evaluate the efficacy of this surgical procedure.

ACKNOWLEDGEMENTS

The authors indicate no source of funding or financial conflict of interest. The authors involved in management, analysis and interpretation, and preparation of the data (MI, HS, RK, KSu) and in interpretation of the data and preparation of the manuscript (MI, KSh, HS, SI). The authors thank Mr Etsuhiko Murakami (Mani Corp, Utsunomiya, Japan) for skilful technical assistance.

REFERENCES

1. De Juan E Jr, Hickingbotham D. Refinements in microinstrumentation for vitreous surgery. *Am J Ophthalmol* 1990; **109**: 218–20.
2. Fujii GY, De Juan E Jr, Humayun MS *et al.* A new 25-gauge instrument system for transconjunctival sutureless vitrectomy surgery. *Ophthalmology* 2002; **109**: 1807–12.
3. Fujii GY, De Juan E Jr, Humayun MS *et al.* Initial experience using the transconjunctival sutureless vitrectomy system for vitreoretinal surgery. *Ophthalmology* 2002; **109**: 1814–20.
4. Ibarra MS, Hermel M, Prenner JL, Hassan TS. Longer-term outcomes of transconjunctival sutureless 25-gauge vitrectomy. *Am J Ophthalmol* 2005; **139**: 831–6.
5. Taylor SR, Aylward GW. Endophthalmitis following 25-gauge vitrectomy. *Eye* 2005; **19**: 1228–9.
6. Liu DT, Chan CK, Fan DS *et al.* Choroidal folds after 25 gauge transconjunctival sutureless vitrectomy. *Eye* 2005; **19**: 825–7.
7. Shimada H, Nakasizuka H, Mori R, Mizukami Y. Expanded indications for 25-gauge transconjunctival vitrectomy. *Jpn J Ophthalmol* 2005; **49**: 397–401.
8. Lopez-Guajardo L, Pareja-Esteban J, Teus-Guezala MA. Oblique sclerotomy technique for prevention of incompetent wound closure in transconjunctival 25-gauge vitrectomy. *Am J Ophthalmol* 2006; **141**: 1154–6.
9. Shimada H, Nakashizuka H, Mori R *et al.* 25-gauge scleral tunnel transconjunctival vitrectomy. *Am J Ophthalmol* 2006; **142**: 871–3.
10. Eckardt C. Transconjunctival sutureless 23-gauge vitrectomy. *Retina* 2005; **25**: 208–11.
11. Yeshurun I, Rock T, Bartov E. Modified sutureless sclerotomies for pars plana vitrectomy. *Am J Ophthalmol* 2004; **138**: 866–7.
12. Kadonosono K, Yamakawa T, Uchio E *et al.* Comparison of visual function after epiretinal membrane removal by 20-gauge and 25-gauge vitrectomy. *Am J Ophthalmol* 2006; **142**: 513–15.
13. Rizzo S, Genovesi-Ebert F, Murri S *et al.* 25-gauge, sutureless vitrectomy and standard 20-gauge pars plana vitrectomy in idiopathic epiretinal membrane surgery: a comparative pilot study. *Graefes Arch Clin Exp Ophthalmol* 2006; **244**: 472–9.
14. Inoue M, Noda K, Ishida S *et al.* Intraoperative breakage of a 25-gauge vitreous cutter. *Am J Ophthalmol* 2004; **138**: 867–9.

Suppression of Choroidal Neovascularization by Inhibiting Angiotensin-Converting Enzyme: Minimal Role of Bradykinin

Norihiro Nagai,[1,2] *Yuichi Oike,*[1,3] *Kanako Izumi-Nagai,*[1,2] *Takashi Koto,*[1,2] *Shingo Satofuka,*[1,2] *Hajime Shinoda,*[1,2] *Kousuke Noda,*[2] *Yoko Ozawa,*[1,2] *Makoto Inoue,*[2] *Kazuo Tsubota,*[2] *and Susumu Ishida*[1,2]

Purpose. Angiotensin-converting enzyme (ACE), also known as kininase II, functions not only to convert angiotensin I to angiotensin II, but also to cleave bradykinin into inactive fragments. Thus, ACE inhibition causes the tissue accumulation of bradykinin, exerting either of two opposite effects: anti- or proangiogenic. The purpose of the present study was to investigate the role of bradykinin in the development of choroidal neovascularization (CNV), with or without ACE inhibition.

Methods. Laser photocoagulation was used to induce CNV in wild-type C57BL/6J mice and angiotensin II type 1 receptor (AT1-R)-deficient mice. Wild-type mice were pretreated with the ACE inhibitor imidapril, with or without the bradykinin B2 receptor (B2-R) antagonist icatibant daily for 6 days before photocoagulation, and the treatment was continued daily until the end of the study. CNV response was analyzed by volumetric measurements using confocal microscopy 1 week after laser injury. The mRNA and protein levels of vascular endothelial growth factor (VEGF), intercellular adhesion molecule (ICAM)-1, and monocyte chemotactic protein (MCP)-1 in the retinal pigment epithelium–choroid complex were examined by RT-PCR and ELISA, respectively.

Results. ACE inhibition led to significant suppression of CNV development to the level seen in AT1-R-deficient mice. B2-R blockade together with high-dose but not low-dose ACE inhibition resulted in more potent suppression of CNV than did ACE inhibition alone. B2-R blockade alone exhibited little or no effect on CNV. VEGF, ICAM-1, and MCP-1 levels, elevated by CNV induction, were significantly suppressed by ACE inhibition. VEGF but not ICAM-1 or MCP-1 levels were further attenuated by B2-R blockade with ACE inhibition.

Conclusions. These results suggest a limited contribution of the kallikrein-kinin system to the pathogenesis of CNV, in which the renin-angiotensin system plays more essential roles for facilitating angiogenesis. The present study indicates the possibility of ACE inhibition as a novel therapeutic strategy to inhibit CNV. (*Invest Ophthalmol Vis Sci.* 2007;48:2321–2326) DOI:10.1167/iovs.06-1296

Age-related macular degeneration (AMD) is the most common cause of blindness in developed countries.[1] It is complicated by choroidal neovascularization (CNV), leading to severe vision loss and blindness. During CNV, new vessels from the choroid invade the subretinal space through Bruch's membrane, resulting in the formation of fibrovascular tissues containing vascular endothelial cells, retinal pigment epithelial cells, fibroblasts, and macrophages.[2] Bleeding and lipid leakage from the immature vessels in the proliferative tissue cause damage to the retinal functions. Molecular and cellular mechanisms for promoting CNV are not fully elucidated. CNV seen in AMD develops with chronic inflammation adjacent to the retinal pigment epithelium (RPE), Bruch's membrane and choriocapillaris. Inflammatory processes including macrophage infiltration[3–6] and the cytokine network[5–7] are associated with CNV, as well as the pathologic angiogenesis seen in solid tumor. Vascular endothelial growth factor (VEGF), a potent proinflammatory and angiogenic cytokine, has been shown to play a central role in CNV.[5–9] VEGF were expressed in both the rodent model of laser-induced CNV[5] and human CNV tissues surgically removed from patients with AMD.[6] VEGF signaling blockade leads to significant suppression of experimental CNV.[7] In accordance with these experimental results, recent clinical trials revealed that intravitreal administration of VEGF antagonists ameliorated the visual outcome compared with sham injections.[8,9] In addition, CNV tissues from both human surgical samples and the rodent laser-induced model express molecules responsible for macrophage infiltration, including intercellular adhesion molecule (ICAM)-1[10,11] and monocyte chemotactic protein (MCP)-1.[2] Genetic ablation of ICAM-1[11] and CCR-2,[4] a receptor for MCP-1, inhibits CNV in a murine model.

The kallikrein-kinin system (KKS) is implicated in various pathologic and physiologic processes, including inflammation, allergy, blood coagulation, and fibrinolysis, and the lowering of systemic blood pressure due to vessel dilation and diuretic action. Bradykinin, the central molecule of the KKS generated by kallikrein from kininogen, induces inflammation via bradykinin B2 receptor (B2-R; Fig. 1) including vessel dilation and leakage.[12] Recent reports[12–15] have demonstrated bradykinin as a positive regulator for angiogenesis, which is shown to depend on B2-R-induced expression of VEGF.[16,17] To date, however, no data have been shown on the role of the KKS in CNV.

The renin-angiotensin system (RAS) plays an important role in the elevation of systemic blood pressure. Angiotensin II, the final product of the RAS generated by angiotensin-converting enzyme (ACE) from angiotensin I, has two cognate receptors, angiotensin II type 1 receptor (AT1-R) and AT2-R.[18] Since the

From the [1]Laboratory of Retinal Cell Biology, the [2]Department of Ophthalmology, and the [3]Laboratory of Vascular Biology and Metabolism, Keio University School of Medicine, Tokyo, Japan.

Supported by Tanabe Seiyaku Co., Ltd., which provided the imidapril.

Submitted for publication October 29, 2006; revised December 18, 2006; accepted February 27, 2007.

Disclosure: **N. Nagai**, Tanabe Seiyaku Co., Ltd. (F); **Y. Oike**, Tanabe Seiyaku Co., Ltd. (F); **K. Izumi-Nagai**, None; **T. Koto**, None; **S. Satofuka**, None; **H. Shinoda**, None; **K. Noda**, None; **Y. Ozawa**, None; **M. Inoue**, None; **K. Tsubota**, None; **S. Ishida**, Tanabe Seiyaku Co., Ltd. (F)

The publication costs of this article were defrayed in part by page charge payment. This article must therefore be marked "*advertisement*" in accordance with 18 U.S.C. §173-i solely to indicate this fact.

Corresponding author: Susumu Ishida, Laboratory of Retinal Cell Biology, Department of Ophthalmology, Keio University School of Medicine, 35 Shinanomachi, Shinjuku-ku, Tokyo 160-8582, Japan; ishidasu@sc.itc.keio.ac.jp.

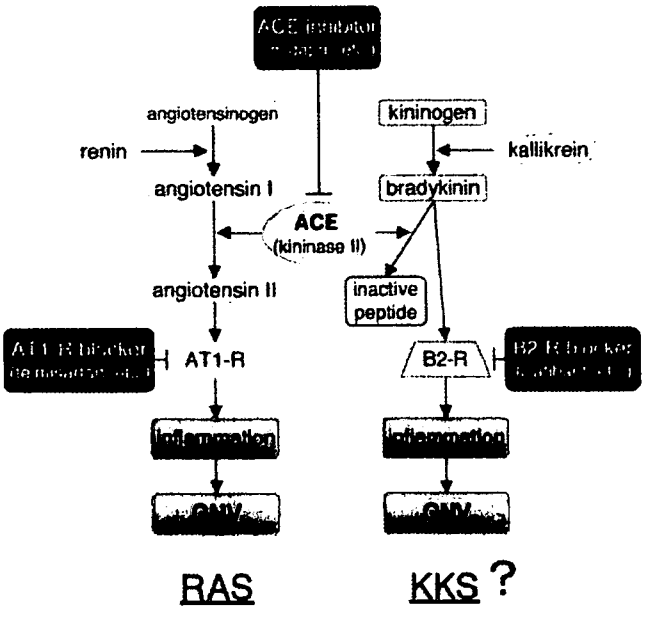

FIGURE 1. Scheme showing the RAS and the KKS components contributing to CNV. Note that inhibition of ACE, also known as kininase II, causes the tissue accumulation of bradykinin, exerting two opposite effects of ACE inhibition: the RAS deactivation leading to antiangiogenic action and the KKS activation leading to proangiogenic action.

major pathogenic signaling of angiotensin II is mediated by AT1-R, ACE inhibitors and AT1-R blockers are widely used in patients with hypertension. In addition, various functions of the RAS have been pointed out, including angiogenesis, inflammation, and tumor growth.[19–21] Recently, we demonstrated that AT1-R, but not AT-2R, blockade led to significant suppression of CNV,[22] providing the first biological evidence of the critical role of the RAS in the pathogenesis of CNV (Fig. 1).

Of note, ACE proved to be an identical molecule with kininase II, which degrades bradykinin to inactive fragments,[12] showing the direct interaction between the RAS and the KKS (Fig. 1). ACE inhibitors, which cause the tissue accumulation of bradykinin,[12] have been shown to be proangiogenic by enhancing the KKS.[23–27] In contrast, ACE inhibitors have also been reported to be antiangiogenic by suppressing the RAS,[28–31] suggesting the tissue specificity of the treatment. However, whether the effect of ACE inhibition on CNV is pro- or antiangiogenic has not been investigated. In the present paper, we defined the effect of ACE inhibition in a murine model of laser-induced CNV. Moreover, the current data are the first to show the role of the KKS in CNV with or without ACE inhibition, together with underlying molecular mechanisms.

MATERIALS AND METHODS

Animals

C57BL/6J mice (7–10 weeks old; CLEA, Tokyo, Japan) and AT1-R-deficient mice (based on the C57BL/6J strain and donated by Tanabe Seiyaku Co., Ltd., Osaka, Japan) were used. All animal experiments were conducted in accordance with the ARVO Statement for the Use of Animals in Ophthalmic and Vision Research.

Induction of CNV

Laser-induced CNV is widely used as an animal model for neovascular AMD and reflects the pathogenesis of CNV seen in AMD. In this model, new vessels from the choroid invade the subretinal space after photocoagulation. Laser photocoagulation was performed around the optic disc at a wavelength of 532 nm, power of 200 mW, duration of 100 ms, and spot size of 75 μm, using a slit lamp delivery system (Novus Spectra; Lumenis, Tokyo, Japan), as described previously.[5]

ACE Inhibition

Animals were pretreated with the ACE inhibitor imidapril or phosphate-buffered saline (PBS) daily for 6 days before photocoagulation, and the treatments were continued daily until the end of the study. Imidapril was the kind gift of Tanabe Seiyaku Co., Ltd. Imidapril was orally administered to mice at a dose of 0.1, 1, 10, or 40 mg/kg body weight.

B2-R Blockade

The B2-R antagonist icatibant (Hoe140; Sigma, St. Louis, MO) was intraperitoneally administered at a dose of 0.1 mg/kg body weight, together with a high (10 mg/kg) or low (1 mg/kg) dose of the ACE inhibitor imidapril, and the CNV volume was analyzed. In addition, icatibant alone at a dose of 0.01, 0.1, or 0.5 mg/kg was administered to mice with CNV. Recently, the phase III clinical trial of icatibant, expected to reduce vascular permeability, for the treatment of hereditary angioedema was successfully completed.

Quantification of Laser-Induced CNV

One week after laser injury, the eyes were enucleated and fixed with 4% paraformaldehyde (PFA). Eye cups obtained by removing anterior segments were incubated with 0.5% fluorescein-isothiocyanate (FITC)-isolectin B4 (Vector, Burlingame, CA). CNV was visualized with a blue argon laser (wavelength, 488 nm) on a scanning laser confocal microscope (FV1000; Olympus, Tokyo, Japan). Horizontal optical sections of CNV were obtained every 1-μm step from the surface to the deepest focal plane. The area of CNV-related fluorescence was measured by NIH Image (available by ftp at zippy.nimh.nih.gov/ or at http://rsb.info.nih.gov/nih-image; developed by Wayne Rasband, National Institutes of Health, Bethesda, MD). The summation of the whole fluorescent area was used as the volume of CNV, as described previously.[5]

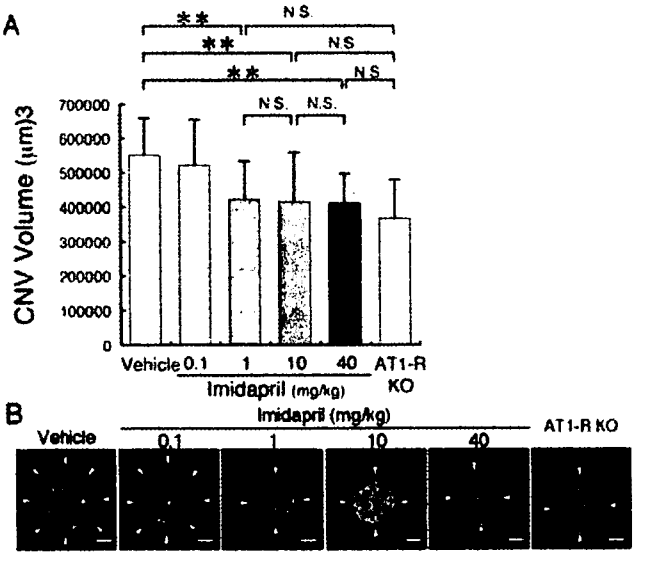

FIGURE 2. Suppression of CNV with ACE inhibition. (A) CNV volume. (B) Flatmounted choroids from vehicle- and imidapril-treated and AT1-R knockout mice. ACE inhibition with imidapril led to significant suppression of CNV to the level of that in the AT1-R knockout mice. *Arrowheads*: lectin-stained CNV tissues. $n = 13$–15. $^{**}P < 0.001$. Scale bar, 50 μm.

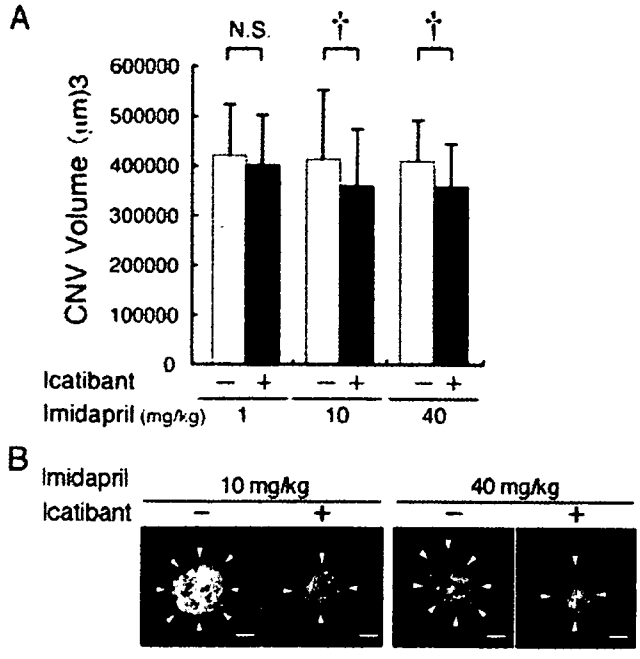

FIGURE 3. Partial role of B2-R in CNV with ACE inhibition. (A) CNV volume. (B) Flatmounted choroids from imidapril- and icatibant-treated mice. B2-R blockade with icatibant, together with high-dose ACE inhibition with imidapril, resulted in more potent suppression of CNV. *Arrowheads*: lectin-stained CNV tissues. $n = 13$–15. $\dagger P < 0.05$. Scale bar, 50 μm.

RT-PCR Analyses for *VEGF*, *ICAM-1*, and *MCP-1*

Total RNA was isolated from the RPE-choroid complex 3 days after photocoagulation using an extraction reagent (TRIzol; Invitrogen, Carlsbad, CA) and reverse-transcribed with a cDNA synthesis kit (First-Strand; GE Healthcare, Buckinghamshire, UK). PCR was performed with *Taq* DNA polymerase (Takara Bio, Ohtsu, Japan) in a thermal controller (Gene Amp PCR system; Applied Biosystems, Foster, CA). The primer sequences and the expected size of amplified cDNA fragments are as follows: 5′-GAA GTC CCA TGA AGT GAT CCA G-3′ (sense) and 5′-TCA CCG CCT TGG CTT GTC A-3′ (antisense) (319 bp and 451 bp) for *VEGF120* and *VEGF164*, respectively; 5′-GTG TCG AGC TTT GGG ATG GTA-3′ (sense) and 5′-CTG GGC TTG GAG ACT CAG TG-3′ (antisense) (505 bp) for *ICAM-1*; 5′-CCC CAC TCA CCT GCT GCT ACT-3′ (sense) and 5′-GGC ATC ACA GTC CGA GTC ACA-3′ (antisense) (380 bp) for *MCP-1*; and 5′-ATG TGG CAC CAC ACC TTC TAC AAT GAG CTG CG-3′ (sense) and 5′-CGT CAT ACT CCT GCT TGC TGA TCC ACA TCT GC-3′ (antisense) (837 bp) for β-actin.

ELISA for VEGF, ICAM-1, and MCP-1

The RPE-choroid complex was carefully isolated from the eyes 3 days after photocoagulation and placed into 200 μL of lysis buffer supplemented with protease inhibitors and sonicated. The lysate was centrifuged at 15,000 rpm for 15 minutes at 4°C, and the protein levels of VEGF, ICAM-1, and MCP-1 were determined with the mouse VEGF, ICAM-1, and MCP-1 ELISA kits (R&D Systems, Minneapolis, MN) according to the manufacturer's protocols.

Morphometric and Statistical Analyses

All results are expressed as the mean ± SD. The data were processed for statistical analyses (Mann-Whitney test). Differences were considered statistically significant at $P < 0.05$.

RESULTS

Suppression of CNV with ACE Inhibition

The CNV volume was measured to evaluate the effects of ACE inhibition with imidapril on the development of CNV (Fig. 2). Imidapril-treated mice at a dose of 1, 10, or 40 mg/kg showed a significant ($P < 0.001$) decrease in the CNV volume (421,630 ± 101,857 μm^3 for 1 mg/kg, 415,041 ± 137,207 μm^3 for 10 mg/kg, and 409,669 ± 87,086 μm^3 for 40 mg/kg) compared with vehicle-treated mice (550,345 ± 108,015 μm^3). The difference in the CNV volume between any dose (1, 10, or 40 mg/kg) of ACE inhibition and AT1-R deficiency (389,132 ± 114,635 μm^3) was not statistically significant.

Partial Role of B2-R Signaling in CNV Development with ACE Inhibition

As the ACE inhibitor-induced suppression of CNV was not in a dose-dependent fashion (Fig. 2), we predicted the possible role of the KKS upregulated by ACE inhibition. Mice receiving the high (10, 40 mg/kg body weight) or low (1 mg/kg body weight) dose of imidapril, both of which significantly suppressed CNV (Fig. 2), were simultaneously administered with the B2-R antagonist icatibant (0.1 mg/kg body weight) (Fig. 3). Icatibant treatment significantly suppressed the CNV volume when cotreated with the high, but not low, dose of imidapril. The CNV volume reduced by the high dose of imidapril (415,041 ± 137,207 μm^3 for 10 mg/kg, 409,669 ± 87,086 μm^3 for 40 mg/kg) was significantly ($P < 0.05$) further attenuated by the simultaneous administration of icatibant (360,936 ± 112,920 μm^3 for 10 mg/kg and 357,958 ± 97,821 μm^3 for 40 mg/kg).

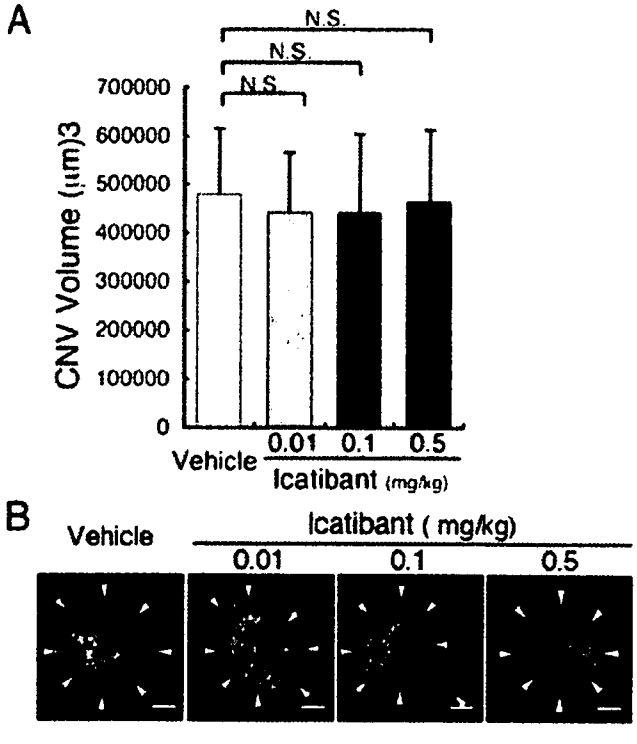

FIGURE 4. Negligible role of B2-R in CNV without ACE inhibition. (A) CNV volume. (B) Flatmounted choroids from vehicle- and icatibant-treated mice. B2-R blockade with icatibant alone exhibited little or no effect on CNV. *Arrowheads*: lectin-stained CNV tissues. $n = 11$–15. Scale bar, 50 μm.

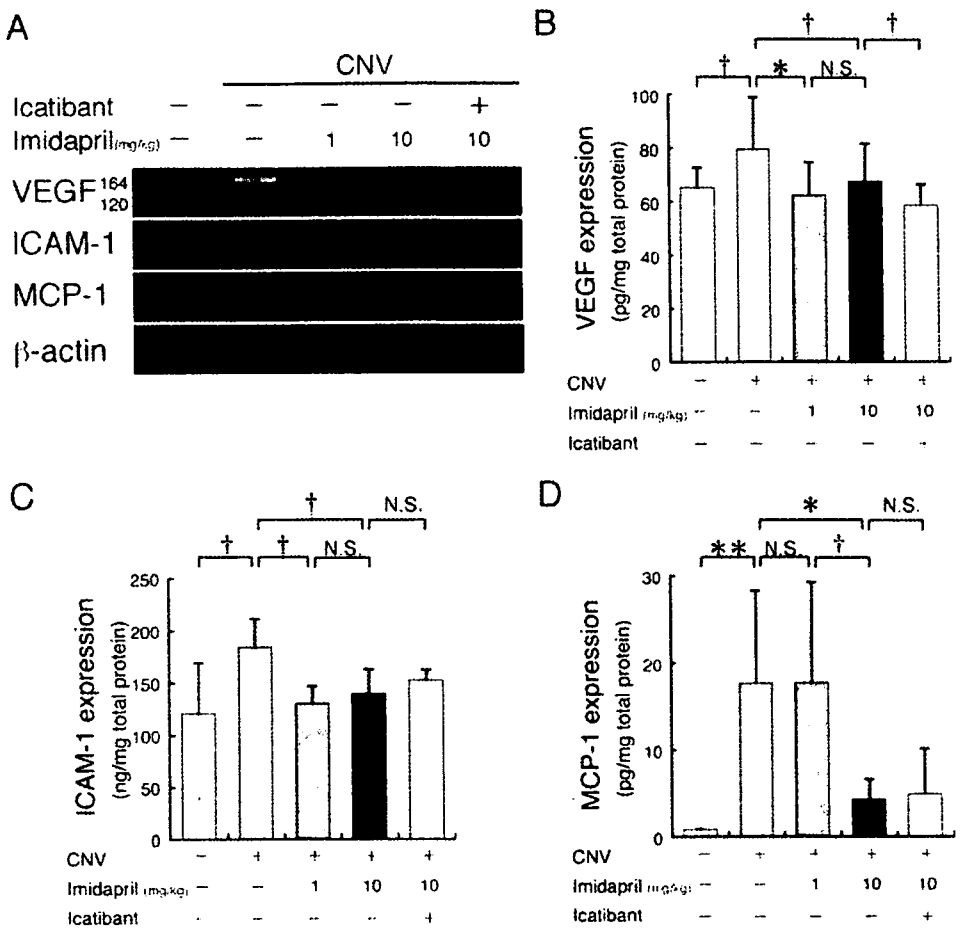

FIGURE 5. Additively suppressive effect of B2-R blockade with ACE inhibition on VEGF, but not ICAM-1 or MCP-1, expression analyzed by semiquantitative RT-PCR (A) and ELISA (B–D). The mRNA expression and protein levels of VEGF, ICAM-1, and MCP-1, elevated by inducing CNV, were significantly suppressed by imidapril. VEGF, but not ICAM-1 or MCP-1, protein levels were further attenuated by the simultaneous administration of imidapril and icatibant. $n = 8$–10. $^*P < 0.01$, $^\dagger P < 0.05$.

Negligible Role of B2-R Signaling in CNV Development without ACE Inhibition

Administration of icatibant alone without ACE inhibition did not significantly change the volume of CNV (450,685 ± 120,616 μm^3 for 0.01 mg/kg, 441,961 ± 162,050 μm^3 for 0.1 mg/kg, and 463,653 ± 148,311 μm^3 for 0.5 mg/kg, $P > 0.05$), compared with vehicle-treated animals (479,393 ± 135,885 μm^3; Fig. 4).

Additively Suppressive Effect of B2-R Blockade with ACE Inhibition on VEGF, But Not ICAM-1 or MCP-1, Expression

To analyze molecular mechanisms in the partial contribution of B2-R signaling to CNV with ACE inhibition, we analyzed the mRNA and protein levels of CNV-related molecules including VEGF, ICAM-1, and MCP-1 in the RPE-choroid complex by semiquantitative RT-PCR (Fig. 5A) and ELISA (Figs. 5B–D), respectively. The mRNA expression and protein levels of VEGF, ICAM-1, and MCP-1 in the RPE-choroid complex were upregulated by inducing CNV. ACE inhibition with systemic administration of imidapril at the dose of 1 or 10 mg/kg body weight significantly reduced the mRNA expression and protein levels of VEGF, ICAM-1, and MCP-1. The B2-R antagonist icatibant further reduced the mRNA expression and protein levels of VEGF, but not ICAM-1 or MCP-1, in the RPE-choroid complex.

DISCUSSION

The RAS and the KKS, each playing an antagonistic role in the regulation of systemic blood pressure, are recently shown as positive modulators of angiogenesis. The present study revealed, for the first time to our knowledge, several important findings concerning the dual contribution of the RAS and the KKS to CNV with ACE inhibition. ACE inhibition led to significant suppression of CNV development to the level seen in AT1-R knockouts (Fig. 2). Notably, the ACE inhibitor-induced suppressive effect on CNV was not in a dose-dependent fashion (Fig. 2). B2-R blockade, together with ACE inhibition resulted in more potent suppression of CNV than ACE inhibition alone (Fig. 3). B2-R blockade alone exhibited little or no effect on CNV (Fig. 4), suggesting a limited contribution of the KKS to the pathogenesis of CNV, in which the RAS plays more essential roles for facilitating angiogenesis. As possible molecular mechanisms, B2-R-mediated upregulation of VEGF, but not ICAM-1 or MCP-1, expression blunted the CNV-reducing effect of ACE inhibition which suppressed these CNV-related molecules (Fig. 5).

Inhibition of ACE, also known as kininase II, has proved to be either proangiogenic by activating the KKS or antiangiogenic by deactivating the RAS, depending on the disease models. ACE inhibition was reported to enhance neovascularization after surgically induced hindlimb ischemia in rabbits,[26] spontaneously hypertensive rats,[27] and mice with[25] or without[25] streptozotocin-induced diabetes. The ACE inhibitor-induced enhancement of hindlimb neovascularization was abolished in B2-R-deficient mice.[23,25] ACE inhibitor treatment also increased cardiac capillary density in spontaneously hypertensive rats, which was diminished by B2-R blockade with icatibant.[24] In contrast, ACE inhibition was reported to suppress neovascularization in the rodent model of oxygen-induced ischemic retinopathy.[28–30] In the murine model of hepatocel-